An Acad Bras Cienc (2020) 92(2): e20200800 DOI 10.1590/0001-3765202020200800
Anais da Academia Brasileira de Ciências | *Annals of the Brazilian Academy of Sciences*
Printed ISSN 0001-3765 I Online ISSN 1678-2690
www.scielo.br/aabc | www.fb.com/aabcjournal

CHEMICAL SCIENCES

An Overview on the Development of Electrochemical Capacitors and Batteries – part II

VITOR L. MARTINS, HERBERT R. NEVES, IVONNE E. MONJE, MARINA M. LEITE, PAULO F.M. DE OLIVEIRA, RODOLFO M. ANTONIASSI, SUSANA CHAUQUE, WILLIAM G. MORAIS, EDUARDO C. MELO, THIAGO T. OBANA, BRENO L. SOUZA & ROBERTO M. TORRESI

Abstract: In the second part of the review on electrochemical energy storage, the devolvement of batteries is explored. First, fundamental aspects of battery operation will be given, then, different materials and chemistry of rechargeable batteries will be explored, including each component of the cell. In negative electrodes, metallic, intercalation and transformation materials will be addressed. Examples are Li or Na metal batteries, graphite and other carbonaceous materials (such as graphene) for intercalation of metal-ions and transition metal oxides and silicon for transformation. In the positive electrode section, materials for intercalation and transformation will be reviewed. The state-of-the-art on intercalation as lithium cobalt oxide and nickel containing oxides will be approached for intercalation materials, whereas sulfur and metal-air will also be explored for transformation. Alongside, the role of electrolyte will be discussed concerning performance and safety, with examples for the next generation devices. Finally, a general future perspective will address both electrochemical capacitors and batteries.

Key words: rechargeable batteries, electrochemical capacitors, electrochemical energy storage, materials for battery electrodes, materials for super capacitors.

INTRODUCTION

In part I of this series of two reviews, we introduced electrochemical energy storage devices, their importance in recent strategies of decentralization of the energy grid and on mobile applications. On top of that, two kinds of devices were highlighted in part I introduction: electrochemical capacitors and batteries. Their main differences were discussed, then part I continued with details of electrochemical capacitors and materials designs for both electrochemical capacitors and batteries. In this part II, more details in batteries operation and different technologies will be presented, and a general future perspective will be given.

BATTERIES

Batteries are another class of electrochemical energy storage device. They contain three key components: a positive electrode, a negative electrode and an electrolyte, similarly to the electrochemical capacitor physical design.

The chemical reaction between the negative electrode and the positive electrode has two components: (i) electronic and (ii) ionic. The ionic component is driven by the electrolyte that forces the electronic component to circulate through an external circuit. Current collectors at the negative and positive electrodes deliver the electronic current to the external circuit. When the potential is sufficiently positive it can extract

electrons from electrode which is compensate by ions from solution. The opposite happens when the potential sufficiently negative, it will inject electrons into the electrode and the movement of ions will also compensate the change in local charge (Goodenough 2013).

The open circuit potential (V_{oc}) can be determined by the difference between the negative electrode chemical potential (μ_-) and the positive electrode potential (μ_+) divided by the magnitude of the electronic charge (e), as shown in equation 1:

$$V_{oc} = (\mu_- - \mu_+)/e \quad (1)$$

The battery's positive and negative voltage limits will depend on the energy gap (E_g) between the HOMO and the LUMO of the electrolyte. μ_- must be lower than the LUMO and μ_+ greater than HOMO of electrolyte, otherwise the electrolyte will be reduced on the negative electrode or oxidized on the positive electrode, forming a passivating solid electrolyte interphase at the negative electrode (SEI) or the cathode electrolyte interphase (CEI) film (Liu et al. 2016a) at the positive electrode, as showed in Figure 1.

During battery operation, some mechanisms behind the electrochemical process occur - the intercalation and the transformation processes. The intercalation process occurs by the insertion of metal ion during charging/discharging processes. During discharge, the ion moves within the electrolyte toward the positive electrode and interleaves into the material. During battery charging, the reverse process occurs, the ion now moves toward the negative electrode, which is the reason why this is known as a reversible process (Figure 2). In contrast to an intercalation material, transformation reactions can also take place in batteries, with the break and formation of chemical bonds during battery charge and discharge.

Rechargeable Batteries

A rechargeable battery makes use of a reversible electrochemical reaction in order to restore the original chemical constitution of electrode components, by means of an electrical current that flows in the opposite direction of the one during discharge. Since this is a non-spontaneous process, an external energy source is required to perform the charge process (Winter & Brodd 2004). Lead-acid, nickel-cadmium and metal-ion are among the most important rechargeable electrochemical systems. This review will focus on metal-ion batteries, especially those based on Li and Na (Silva et al. 2016).

Metal-ion batteries

Metal-ion batteries are based on the ion insertion/extraction into/from electrodes, and include Li^+, Na^+, Mg^{2+}, and Al^{3+}, being increasingly researched in both academy and industry. Among these metal-based systems, lithium has emerged as the battery of choice for both higher energy density and lighter weight. Since production capability became available, Li-ion batteries rapidly replaced the Ni-MH batteries (Liu et al. 2016a). Details concerning

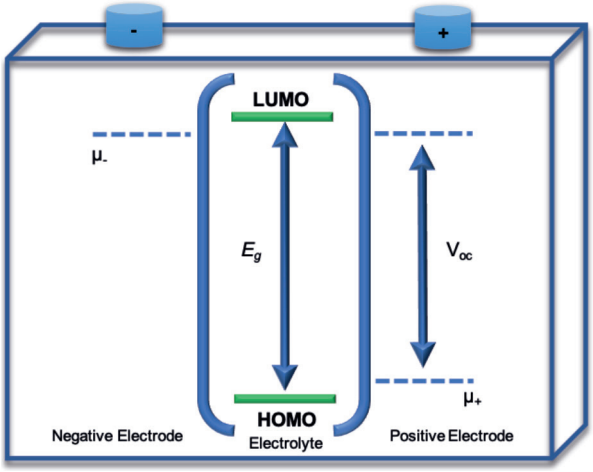

Figure 1. Scheme showing energy diagrams of LUMO and HOMO of the electrolyte, and the electrochemical potential of each of the electrodes in a battery.

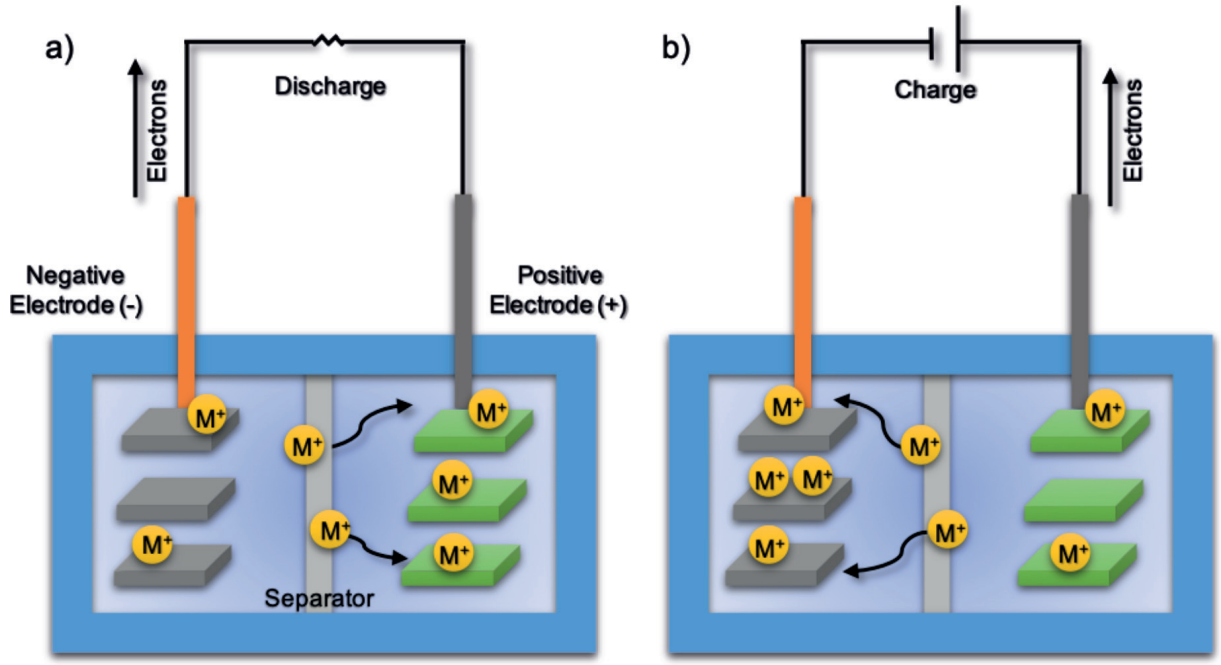

Figure 2. Schemes of metal-ion batteries discharge (a) and charge (b) processes.

electrochemical mechanism, components constitution and materials properties will be further discussed, divided in negative electrodes, positive electrodes and electrolytes.

Negative electrodes

The negative electrode material is the one that carries the electrons to the external circuit and oxidizes during the electrochemical reaction. In a battery case, at the negative electrode, an oxidation reaction occurs during discharge. The process is reversed during charge, when a reduction reaction occurs allowing lithium or sodium ions to enter by different ways (intercalation into a crystalline structure or transformation forming Li_2O or Na_2O). In most cases, the potential is so low that electrolyte reduction can take place, forming a film. However, the formation of this surface film, which is electronically insulating but ionically conductive, stops further decomposition of the solvent but allows the electrochemical process of metal ion insertion to continue. The research and understanding of the characteristics of negative electrode interfaces were particularly promoted by the pioneering work of Peled et al. (1995), who called this passivation layer SEI, and later by Jeong et al. (2001), who demonstrated its formation, and have been of fundamental importance for the understanding of battery electrode processes. We are looking for the lower working potential with a greater cell voltage and consequently a higher battery energy density.

Metallic

The ideal negative electrode for lithium batteries is undoubtedly, metallic lithium, since it presents enormous theoretical specific capacity (3860 mA h g^{-1}), low density (0.59 g cm^{-3}) and low working potential (-3.04 V vs SHE). On the other hand, rechargeable batteries based on metallic lithium negative electrodes are not commercialized due to a practical problem: dendrites are formed during numerous charge/discharges cycles, which can result in loss of metallic lithium (low coulombic efficiency) and generation of internal

short circuits affecting battery safety and cycle life (Figure 3) (Shen et al. 2018).

On the other hand, sodium metal has a much lower specific capacity, only 1165 mA h g^{-1}, due to its higher mass in comparison to lithium. Its working potential is also smaller, being -2.71 V vs SHE. However, the element's availability has made it be studied as a battery negative electrode since the 1960s (Zheng et al. 2019). The issues to be overcome for the commercializing of sodium metal negative electrodes are similar to those of lithium but aggravated by the high reactivity of sodium. The SEI layer is unstable and re-grown in every cycle below 1 V vs Na/Na^+, causing low coulombic efficiency, gas evolution, and electrolyte exhaustion that eventually leads to cell failure (Lee et al. 2019). Moreover, sodium plating is also accompanied by dendritic growth (Zheng et al. 2019). New insights on the stabilization of the SEI layer and the use of solid electrolytes (Gao et al. 2018) have been investigated in order to make metal sodium negative electrodes safe and efficient.

In this review we approach two possible strategies for replacing lithium or sodium metal negative electrodes in order to overcome the aforementioned safety problems. In the last decades, a series of alternatives have been investigated, and they can be divided into two main types: lithium/sodium-ion intercalation or insertion materials and transformation materials. However, new knowledge is necessary to build better lithium negative electrodes, since there are two kinds of next-generation batteries with high-energy-density which are those Li-S and Li-Air. For sodium-ion batteries (SIBs), the technology is still at an early stage and multiple materials are still being introduced as negative electrodes.

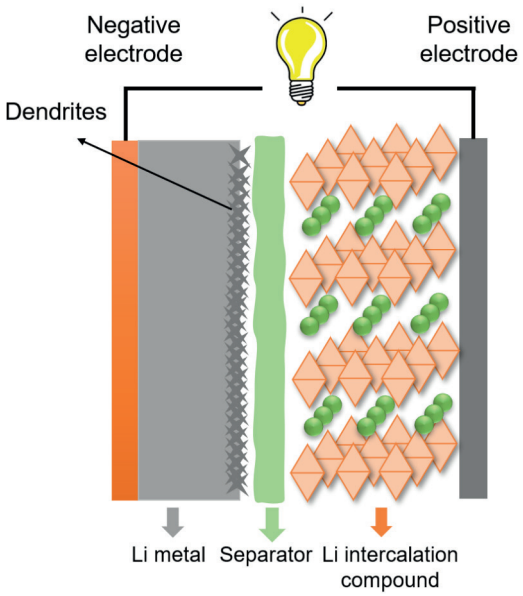

Figure 3. Schematic diagram of a Li-metal battery with a Li-intercalation material as positive electrode and a separator soaked with electrolyte, showing the formation of Li dendrites on the negative electrode.

Intercalation

In order to identify materials that could resist long-lasting cycling but avoiding the deposition of metallic lithium, lithium-ion insertion materials (or intercalating electrodes) were developed in 1978 by M. S Whittingham, to be used as positive electrodes. They are compounds that can reversibly incorporate and release lithium ions from their open structure, and at the same time assume different oxidation states (Whittingham 1978). These conditions are satisfied by carbon-based materials (e.g. graphite) and transition metal compounds among others.

Carbon-based materials

The use of graphite as a negative electrode can be considered the key advance that opened the way to commercial lithium-ion batteries (LIBs). Indeed, the choice of graphite as a negative electrode is quite surprising, since the electrochemical intercalation of lithium ions

takes place outside the stability window of most organic solvents. The solvent, as we described above, decomposes on the graphite surface during the reduction (discharge) process, forming the SEI, when electronic charge is stored in the graphite network while lithium ions are inserted between the carbon sheets. Therefore, graphite is thermodynamically unstable but kinetically protected. The correct use of graphite as negative electrode in LIBs applications was demonstrated by Jeong et al. (2001). However, 10 years before the concept had reached a practical application with a battery introduced by Sony in 1991 (Blomgren 2017). The key feature of Sony's battery, called "lithium-ion battery" was the choice of suitable electrode materials, using graphite as a negative electrode and a cobalt and lithium oxide ($LiCoO_2$) as a positive electrode, as proposed by Yoshino (2000) and Mizushima et al. (1980) in Goodenough's group, respectively. In the present, many studies have been made to improve the life-cycling of graphite. For instance, recently Chen et al. (2018) have investigated a modification of a typical synthesis of graphite by microwave irradiation. The authors inform a long-cycling performance of 410 cycles obtaining 370 mA h g^{-1}, which corresponds to a 99.46% of the theoretical capacity. They associate this important improvement to the state-of-the-art in graphite negative electrodes to the formation of nano-graphite starting from flake graphite and expanded graphite edge as well as a stable SEI formation.

Although graphite is the state-of-the-art negative electrode in LIBs, it presents a low specific capacity towards sodium-ion intercalation (30 mA h g^{-1}) (Xu et al. 2019b). This is because the formation energy of NaC_x is energetically unfavorable (Lenchuk et al. 2019, Li et al. 2019b, Liu et al. 2016c, Moriwake et al. 2017). A few groups have been working on tuning the electrolyte solvent as an approach to increase graphite capacity toward sodium-ion intercalation (Goktas et al. 2018, Jache & Adelhelm 2014, Xu et al. 2019b). Hard carbons, on their turn, have specific capacities varying from 100 to 300 mA h g^{-1}, depending on their structure. They are considered disorganized forms of carbon. If the structure can be transformed into graphite (organized) under high temperature, the material is said to be non-graphitic. If the disorganized form is the most thermodynamically stable structure at all temperatures, the material is considered non-graphitizable (Dou et al. 2019). Their structure can be described as composed of fragments of bundled non-planar graphenic sheets, where graphene layers are locally stacked by van der Waals forces (Dou et al. 2019). Hard carbons are commonly obtained by controlled pyrolysis of organic compounds, which include polymers and biomass (Baldinelli et al. 2018). The process can lead to highly porous carbons with high surface area. The possibility to use biomass waste as carbon source makes of hard carbons a cheap and sustainable option for SIB negative electrodes. However, it requires care, since composition and homogeneity of precursor materials are a key factor affecting structure and properties of the obtained hard carbon (Dou et al. 2017, Gomez-Martin et al. 2019). Table I shows different hard carbons used as SIB negative electrodes from works published in the past year. For more examples, specific reviews on hard carbons can be found in references (Dou et al. 2019, Hou et al. 2017, Xiao et al. 2019).

The mechanism of sodium ions intercalation in hard carbons is still under debate (Anji Reddy et al. 2018, Dou et al. 2019, Gomez-Martin et al. 2019). During discharge, there is a sloping line between 1.2 V and 0.1 V, and a plateau at very low potentials (<0.1 V vs Na/Na^+). The mechanism has been described as a "falling cards" model (Dahn et al. 1997), where first there would be

Table I. Electrochemical performances of different hard carbons for SIBs.

Precursor	Pyrolysis conditions	Specific Capacity (mA h g^{-1})	Reference
Pectin-free apple pomace	1100 °C / Argon / 1h	285 at 0.2 A g^{-1}	(Dou et al. 2018)
Sepals of Palmyra palm fruit	700 °C / Argon / 2h	275 at 0.3 A g^{-1}	(Damodar et al. 2019)
Sucrose/Graphene Oxide	1100 °C / Argon / 6h	220 at 0.2 A g^{-1}	(Luo et al. 2015)
Templated glycine	790 °C / NH_3 flow / 2h	265 at 0.1 A g^{-1}	(Hu et al. 2019)
Bacterial cellulose	1300 °C / Argon / 6h	233 at 0.2 A g^{-1}	(Yang et al. 2019b)

sodium insertion in disordered carbon layers (sloping line region) and then the adsorption of sodium into the material's nanopores (plateau region). The oxidation state of adsorbed sodium in the plateau region has been observed as zero (metallic sodium) (Stevens & Dahn 2000) or nearly zero (Stratford et al. 2016). Although the very low insertion potential is an advantageous property of hard carbons, it also brings safety concerns. At high charge/discharge rates, it could cause irreversible sodium plating.

Not long ago, with the discovery and development of graphene plus the numerous reports of improved active materials for positive and negative electrodes modified with graphene, many researchers started believing that the capacity of LIBs can only be enhanced significantly by replacing the typical graphite negative electrode by pure graphene. This material shows superior conductivity (compared to metal), high surface area (2630 m^2 g^{-1}), and would present the possibility of incorporating lithium on both faces of the sheets (forming the Li_2C_6 stoichiometry with a theoretical specific capacity of 744 mA h g^{-1}). Nevertheless, despite the considerable investment of money and time, this goal has not been achieved for pure graphene materials. The mechanism of lithium incorporation on single-layer graphene is still under debate both experimentally and theoretically (Ji et al. 2019, Kühne et al. 2017, Lee & Persson 2012). For instance, Pollak et al. (2010) studied the interaction between lithium ions and a single-layer graphene (SLG) and few-layers graphene (FLG). The authors found that the carbon-Li interaction in FLG resembles that of typical bulk graphite, while SLG performs radically differently, without the formation of the common stage 1 of LiC_6 phase. They associate this behavior to lower binding energies of lithium to carbon and strong Coulombic repulsion of the lithium atoms on the opposite sides of the graphene, leading to low surface coverage of SLG. Furthermore, Ji et al. (2019) found that there is no significant difference between bilayer graphene, FLG and graphite electrodes in the Li-storage mechanisms and kinetics behavior. Therefore, the use of graphene as a negative electrode for LIBs is controversial.

The adsorption of Na^+ ions onto the surface of pure SLG, as onto graphite, is energetically unfavorable according to theoretical studies (Yoon et al. 2017). Experiments also have shown the poor performance of SLG in SIBs: the capacity of SLG electrodes was very close to that of the bare copper foils on which SLG was grown by CVD (Ramos et al. 2015). However, the high theoretical capacity (300 – 500 mA h g^{-1}) arising from the possibility of incorporating Na^+ to both the sides of graphene sheets (Zhang et al. 2020) encourages the search for modifications of graphene electrodes that could change the energetics of the graphene-Na^+ interaction. For instance, Yang et al. (2017b) have studied two different types of defects, protrusions and holes, created by doping multi-layer graphene

with P and N, respectively. P-doped graphene (with protrusions) achieved a capacity of 350 mA h g^{-1} at 50 mA g^{-1}, while nitrogen-doped graphene (with holes) showed a capacity of 211 mA h g^{-1} at the same rate.

Despite the efforts aforementioned, the main use of graphene in battery electrodes is in the form of composites with an electroactive material. Associating a graphene framework to materials such as nanostructured transition metal oxides can lead to electrodes which are chemically more stable, with better mechanical properties, and higher electrical conductivity (Wang et al. 2020).

Alkali titanates

Lithium titanate, $Li_4Ti_5O_{12}$ (LTO), is a material that uses titanium oxide as raw material and results of great interest to be employed as negative electrode for LIBs. LTO has the property of (de) intercalating reversibly up to 3 lithium ions per formula at 1.55 V vs. Li/Li^+, with a theoretical capacity of 175 mA h g^{-1} according to the equation 2:

$$Li_4Ti_5O_{12} + 3\ Li^+ + 3\ e^- \rightleftarrows Li_7Ti_5O_{12} \quad (2)$$

This reaction occurs at higher potentials than that of the decomposition of organic solvents and consequently there is no formation of a SEI layer. LTO presents interesting properties in terms of long-life cycling of charge/discharge in comparison with other negative materials. In addition, LTO is considered a *zero strain* material, due to the negligible structural change during the charge/discharge process (a reduction of the unit cell of only 0.2%). For instance, Chauque et al. (2017) showed the impact of a ball-milling treatment on the structure and crystallinity of LTO and its energy storage. The authors tried to decrease the particle size of LTO (synthesized by a typical ceramic method at 950 °C) in order to improve the diffusion path of lithium ions. The use of high-energy milling for different times showed that the specific capacity increased as the particle size decreased. But when the ball-milling applied time affected the crystallinity of the LTO, the capacity decayed drastically. However, the addition of graphite to LTO during grinding showed an improvement on specific capacity and rate capability response as well as a higher diffusion coefficient. Another example of the use of LTO as negative electrode is provided by Kim et al. (2017) who focused on improving the low electronic conductivity of LTO by adding graphene. The authors prepared a single-layered graphene-wrapped LTO (~200 nm) with a specific capacity of 130 mA h g^{-1} at high current densities of (de)lithiation of 30 C (1 C rate is the necessary current to charge/discharge the battery full capacity in one hour). The authors associate the remarkable performance to the improvement of the electronic conductivity of the final composite being ca. 1.6 x 10^{-3} S cm^{-1}. The use of LTO as a negative electrode for LIBs application is closely linked to its great stability during numerous cycles of charge and discharge even at high current densities. However, it is still limited due to its high potential plateau (1.55 V vs. Li/Li^+) as well as low specific capacity compared to graphite or transformation materials.

For SIBs, the semiconductor layered sodium trititanate $Na_2Ti_3O_7$ (NTO) draws attention for its low sodium-ion insertion potential of 0.3 V vs Na/Na^+ (Senguttuvan et al. 2011). Its theoretical specific capacity is 178 mA h g^{-1} with the uptake of two sodium ions per formula unit and reduction of 2/3 of Ti^{4+} to Ti^{3+}, according to equation 3 (Senguttuvan et al. 2011). The compound consists of a layered zig-zag structure of $[TiO_6]$ octahedra with sodium ions occupying sites in the interlayer region. Similar to other sodium titanates (Andersson & Wadsley 2002), NTO is interesting due to its low toxicity, high availability of precursor materials (TiO_2 and Na

compounds), and easy fabrication. However, the semiconductor has low electronic and ionic conductivity. The addition of carbon as particle coating (Hwang et al. 2019) or composites (Yan et al. 2015, Zhou et al. 2016) is a common method to improve the electronic conductivity. Nanostructuring NTO into nanosheets or nanotubes by an alkaline hydrothermal method (Anwer et al. 2017, Kasuga et al. 1998, Ko et al. 2017, Wang et al. 2015b) showed an improved performance at high rates due to the higher contribution of surface process in the overall electrode response (Leite et al. 2020).

$$Na_2Ti_3O_7 + 2Na^+ + 2e^- \rightleftarrows Na_4Ti_2^{3+}Ti^{4+}O_7 \quad (3)$$

Transformation

To replace the current intercalation-type negative electrode materials, conversion-type electrode materials are very promising because of their high theoretical capacity and low working potential. Among the candidates that have been reported in bibliography, we highlight two ways to incorporate lithium or sodium: the iron oxides (such as Fe_3O_4) and the formation of lithium (or sodium)-alloys (i.e. silicon).

Iron Oxides

Transition metal oxides (TMOs) can be reduced with concomitant lithium participation to maintain electroneutrality, as shown in the following conversion-type reaction in equation 4:

$$M_xO_y + 2yLi^+ + 2ye^- \rightleftarrows xM^0 + yLi_2O \quad (4)$$

where M is a transition metal that can deliver high specific capacities, much higher than graphite. Fe_3O_4 (magnetite) has long been considered a promising negative electrode material due to its high theoretical capacity (934 mA h g^{-1}). In Table II, we summarize some previously published works, remarking the specific capacities obtained as well as the number of cycles performed.

The insertion of sodium in conversion-type materials usually causes higher volume expansion than lithium (Nayak et al. 2018) going up to 250% (Klein et al. 2013), but the high theoretical capacity associated to the process makes of these materials promising alternatives to sodium metal. Only a few oxides have been explored, mainly CuO (Klein et al. 2017), NiO (Hasa et al. 2015) and Fe_2O_3 (Hasa et al. 2015, Li et al. 2017a, Valvo et al. 2014), with theoretical capacities of 674, 718 and 1007 mA h g^{-1}, respectively. To avoid electrode pulverization caused by the large volume change, nanostructuring, doping and hybridization with conductive carbon (Deng et al. 2018) are some electrode modifications that can be approached.

Alloys compounds

Silicon, having a theoretical specific capacity around 10 times larger than that of the state-of-the-art graphite, has been regarded as one of the most promising materials for the next generation of LIBs. The Li-Si alloy with the highest lithium concentration, the $Li_{22}Si_5$ phase with a theoretical specific capacity around 4200 mA h g^{-1}, is more Li-rich than fully lithiated graphite LiC_6 (372 mA h g^{-1}) (Zhang et al. 2016b). Nevertheless, the process of commercializing silicon as a negative electrode is not straightforward due to two important drawbacks: 1) Pulverization of silicon particles (mainly in those with particle size above 150 nm) as a consequence of silicon volume expansion upon lithiation process and the resultant loss of electrical contact (Liu et al. 2012); 2) the continue formation a fresh SEI layer upon cycling (Andersen et al. 2019).

To date, tremendous effort has been made to overcome these problems. For example, strategies such as nanostructured silicon, i.e. nanowires, hollow nanostructures, and clamped hollow structures, Si–C yolk–shell structures (Liu et al. 2014a, Wu et al. 2012a, Wu & Cui 2012),

Table II. Electrochemical performances of different Fe_3O_4.

Material	Specific capacity at 0.1 A g^{-1} (mA h g^{-1})	Cycle number	Reference
Fe_3O_4@C NPs	500	100	(Ma et al. 2017a)
Fe_3O_4-G2	845	150	(Bracamonte et al. 2017)
N-G-Fe_3O_4	800	100	(Liu et al. 2014b)
G-Fe_3O_4-GNRs	796	300	(Li et al. 2015a)
Fe_3O_4/GN(15%)	825	100	(Jiao et al. 2016)
Fe_3O_4@N-doped graphene	850	200	(Chauque et al. 2020)

coatings (Piper et al. 2013, Wu et al. 2012b) and binders (Assresahegn & Bélanger 2017, Koo et al. 2012) have been studied and significant improvement has been seen. The silicon-oxide family (in which oxides such as SiO, SiO_2, non-stoichiometric SiO_x and Si-O-C are included) is an interesting alternative due to its low cost, easy synthesis and small volume change during cycling compared to silicon. In the case of SiO_x, its main outstanding property is its theoretical specific capacity in the fully lithiated phase, which is 3172 mA h g^{-1}. However, these kinds of materials suffer from poor electrical conductivity, in addition to the fact that their initial Coulombic efficiency (ICE) is around 50-80% in the bare SiO_x. This low ICE is a consequence of the formation of lithium oxide (Li_2O) and Li silicate (Li_4SiO_4) in the first cycle, which is considered an irreversible transformation (Chen et al. 2017).

Among the strategies to overcome these drawbacks are the use of carbon as coating or incorporating different carbon sources during the synthesis of silicon oxide materials. For instance, in SiO_x/C hybrids materials, sol-gel of siloxanes (e.g. tetraethoxysilane (TEOS), 1,3,5,7-tetramethyl-1,3,5,7-tetravinylcyclotetrasiloxane (TTCS), hydrogen silsesquioxane) have been widely used. For example, David et al. (2016) synthesized SiO_x/C composites by mixing SiOC with graphene at different ratios. The electrode with a 60:40 ratio (SiOC:graphene) delivered a charge capacity of 588 mA h g^{-1} at 0.1 A g^{-1} and a capacity of 200 mA h g^{-1} at high current (1.6 A g^{-1}). Moreover, the 3D porous reduced graphene structure around the SiOC acts as an effective current collector and electron conductor. Similarly, in order to improve the electrochemical performance of SiO_x Li et al. (2015b) reported a route to anchor the SiO_x-C on the surface of graphene nanoplatelets (GNPs). The derived SiOx-C/graphene nanoplatelets composite showed that the capacity remained above 600 mA h g^{-1} at 0.1 A g^{-1} after 250 cycles, higher than that of 380 mA h g^{-1} for the bare SiO_x-C.

Some relevant electrochemical performances of the above-mentioned materials and other silicon-based/C composites are shown in the Table III.

There are others strategies to improve ICE, as pre-lithiation of the silicon-based anode and the replacement of polymeric binder (in electrode formulation) and electrolyte (Liu et al. 2019b). In the case of pre-lithiation, which refers to the addition of active lithium to the cell before operation, Yoo et al. (2018) were able to improve the low ICE of 2D nanostructured Si/SiO_x from 33% to 82% after a pre-lithiation of 6 hours. By this means, the inserted lithium ions can compensate the active lithium loss, e.g. caused by SEI formation, which leads to a reduction of the first cycle capacity loss

Table III. Electrochemical performances of Si-C and SiO_x-C composites.

Material	Specific capacity (mA h g^{-1})	Current density (A g^{-1})	Cycle number	Reference
Si/SiOx nanofoils	650	50	200	(Yoo et al. 2018)
SiOC	200	1.6	1600	(David et al. 2016)
SiOx-C/GNPs	630	0.1	250	(Li et al. 2015b)
SiOx/C	674.8	0.1	100	(Wu et al. 2015b)
Si/SiOx/C	726	0.1	500	(Qian et al. 2017)
SiOx/C dual-phase	840	0.1	100	(Lv et al. 2015)
Nano-Si/C	878.6	0.12	150	(Pan et al. 2016)
Si-C/G	1020	0.2	100	(Wu et al. 2015a)

(Holtstiege et al. 2018). Sanchez-Ramirez et al. (2020) synthesized new electrolytes that allow to achieve an ICE higher than 70% with average and Columbic efficiencies close to 100% after 1000 cycles in silicon/polyacrylonitrile electrodes. The [FSI]-based ionic liquids (bis(fluorosulfonyl) imide anion) formed a more stable SEI layer because of the presence of [FSI] anions, which act not only as counter ions but also as additive (Piper et al. 2015). With continuous and intensive worldwide efforts, we may expect significant advances in the application of silicon and SiO_x materials in the near future.

Silicon could form a NaSi alloy with a theoretical capacity of 954 mA h g^{-1} at very low potentials vs Na/Na^+ (Nayak et al. 2018). However, crystalline silicon has limited sodium storage ability (Song et al. 2019b). Amorphous silicon, on the other hand, was shown to produce a specific capacity of 240 mA h g^{-1} after 100 cycles when used as a 50 nm thick film (Jangid et al. 2017). In comparison, tin (Sn) is a more promising material for sodium energy storage, having a theoretical capacity of 847 mA h g^{-1} with the uptake of 3.75 Na per Sn ($Na_{15}Sn_4$) (Song et al. 2019b). A study has demonstrated that the electrode suffers from a higher volume expansion upon sodiation than upon lithiation. However, in the opposite process, (de)lithiation causes pulverization of the material while (de)sodiation promotes a microstructural stabilization that could make the technology viable (Wang et al. 2015a), but still with the need to overcome the problems of a large volume change during the (de)sodiation process. Nanostructuring and/or encapsulating Sn particles are useful approaches to prevent electrode pulverization. For example, Sn nanodots (1-2 nm particles) encapsulated in carbon nanofibers delivered a capacity of 633 mA h g^{-1} at 0.2 A g^{-1} (Liu et al. 2015). Another approach to improve Sn electrode performance is tuning the electrolyte. Ether-based electrolytes such as glyme (Zhang et al. 2016a) seem to have an effect on stabilizing Sn electrodes for thousands of cycles (Kim et al. 2018). Other materials, such as antimuonium (Darwiche et al. 2012) and phosphorus (Zhang et al. 2019), also have been contemplated as alloying-type negative electrodes for SIBs. Although these materials show very high capacities in comparison to intercalation materials, to make them viable for commercialization is still challenging. More research on SIB electrodes is needed in order to have better understanding of the involved mechanisms and how to improve the overall electrode performance.

Positive Electrodes

Intercalation

A large number of lithium compounds began to emerge, intercalation components, elements forming alloys with metal or transformation materials. In general, the intercalation compounds are mostly layered oxides and polyanionic materials. Currently, all of them rely on redox chemistry of active transition metals, forming a reversible host structure for lithium intercalation (Grimaud et al. 2016, Huang et al. 2018). The most used positive electrodes in Li-ion batteries are layered $LiCoO_2$ (LCO) made in 1980 (Mizushima et al. 1980), $LiNiO_2$ (LNO) (Rougier et al. 1996), $LiNi_xMn_yCo_zO_2$ (NMC or NCM) (Bak et al. 2014) with different stoichiometries, layered $LiNi_{0.8}Co_{0.15}Al_{0.05}O_2$ (NCA), spinel $LiMn_2O_4$ (LMO) designed in 1983 (Thackeray et al. 1983, 1984), the olivine's family $LiMPO_4$ (M = Fe, Mn.) reported in 1997 (Padhi, 1997), and tavorite, with specific capacities around 200 - 300 mA h g^{-1} (Wu & Yushin 2017). Figure 4 shows the capacity and operating potential for these classes of materials.

Considering layered compounds, LCO is the most used intercalation material. Cobalt and lithium are at octahedral sites in alternating layers and form a hexagonal symmetry. The LCO has a high theoretical specific capacity of 274 mA h g^{-1} and a volumetric capacity of 1363 mA h cm^{-3}, a high discharge voltage of 3.8 V, a robust cycle performance and reduced self-discharge (Cho et al. 2003). To reduce costs, LNO was proposed but it did not show improvement regarding specific capacity. Furthermore, Li^+ tends to replace Ni^{2+} sites during the process of synthesis and deletion, blocking Li^+ diffusion pathways (Rougier et al. 1996). Replacing Co with Mn could be an interesting idea due to lower toxicity and low cost. But there are some problems: (i) dissolution of Mn occurs when

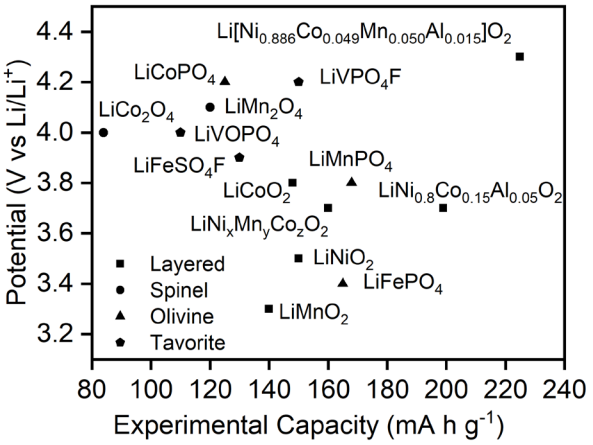

Figure 4. Experimental specific intercalation capacity of positive materials. $LiCoO_2$ (Cho et al. 2003); $LiNiO_2$ (Rougier et al. 1996); $LiMnO_2$ (Bruce et al. 1999); $LiNi_xMn_yCo_zO_2$ (Bak et al. 2014); $LiNi_{0.8}Co_{0.15}Al_{0.05}O_2$ (Martha et al. 2011); $LiMn_2O_4$ (Thackeray et al. 1984); $LiCo_2O_4$ (Choi & Manthiram 2002); $LiFePO_4$, $LiMnPO_4$ and $LiCoPO_4$ (Nitta et al. 2015); $LiVPO_4F$, $LiVOPO_4$ and $LIFeSO_4F$ (Li et al. 2017b).

transformed into Mn^{3+}, and the compound is disproportionated into Mn^{2+} and Mn^{4+} in all Mn-positive electrodes. (ii) during cycling, Mn at LMO can leach out, and (iii) the layered structure tends to convert into a spinel structure during the delithiation. Furthermore, Mn solubilization can lead to a SEI destabilization at the negative electrode (Armstrong & Bruce 1996, Gu et al. 2012, Tu et al. 2006). The NMC formed by Li/Ni/Mn/Co has a theoretical specific capacity of 280 mA h g^{-1}, similar to LCO, but the cost is reduced due to the lower amount of cobalt. One of the most used NMC is the $LiNi_{0.33}Co_{0.33}Mn_{0.33}O_2$ (Bak et al. 2014) Swapping manganese for aluminum gives NCA Li/Ni/Al/Co with specific theoretical capacities similar to LCO, but they degrade at lower temperatures (Martha et al. 2011).

Recently, several new types of lithium intercalation materials for positive electrodes with higher capacities have been developed. Kim et al. (2019) developed a hybrid positive electrode NCA-NCMA90 ($Li[Ni_{0.886}Co_{0.049}Mn_{0.050}Al_{0.015}]O_2$ formed by a core of $Li[Ni_{0.934}Co_{0.043}Al_{0.015}]$

O_2 encapsulated by $Li[Ni_{0.844}Co_{0.061}Mn_{0.080}Al_{0.015}]O_2$. This core@shell structure provided an exceptionally high discharge capacity of 225 mA h g^{-1} at 4.3 V and 236 mA h g^{-1} at 4.5 V, which are better values than the separated NCM and NCA electrodes. The authors believe that the ordering of Li ions in the new hybrid on a microscopic scale led to a stabilization of the host structure during the cycles and facilitated Li^+ intercalation. To try to increase the electrochemical performance, Liu et al. (2019a) developed a material from ($Li_{1.2}Ni_{0.2}Mn_{0.6}O_2$) doping with Cr ($Li_{1.2}Ni_{0.16}Mn_{0.56}Cr_{0.08}O_2$) and finally coating with $LiAlO_2$. The 3 wt % $LiAlO_2$-coated LNMCr showed the highest discharge specific capacity of 268.8 mA h g^{-1} and the best cycling stability among different coating levels (1, 3 and 5 wt %) compared with pristine $Li_{1.2}Ni_{0.2}Mn_{0.6}O_2$ (230.4 mA h g^{-1}) and Cr-doped $Li_{1.2}Ni_{0.16}Mn_{0.56}Cr_{0.08}O_2$ (248.6 mA h g^{-1}). The higher lithium ion diffusion coefficient contributed to the excellent rate capability.

There are many compounds in the spinel family, presenting many stable and robust materials. Spinel $LiMn_2O_4$ was developed and commercialized since 1980s, and it stands out due to the high theoretical specific capacity of 148 mA h g^{-1}. Li is located in tetrahedral 8a sites and Mn in octahedral 16d sites in a ccp matrix of oxygen anions. The lithium ion can diffuse through the vacancies of these interstitial sites (Nitta et al. 2015, Thackeray et al. 1984). Recently, Huang et al. (2018) reported the synthesis and electrochemical application of hybrid spinel/layered oxide ($Li_{1.15}Ni_{0.20}Mn_{0.87}O_2$) as a superior positive electrode. The synergistic effect of nanostructure and spinel/layer heterostructure enhances charge transfer, lithium ion diffusion, and structural stability, resulting in improved ICE (near 100%), reversible capacity (150 mA h g^{-1} at 5 C), and good cyclability (258 mA h g^{-1} after 70 cycles at 0.2 C).

In a similar strategy, Ge et al. (2019) developed an integrated layered-spinel material with a composition of $0.2LiNi_{0.5}Mn_{1.5}O_4.0.8Li[Li_{0.2}Ni_{0.2}Mn_{0.6}]O_2$ at various temperatures. The spinel phase of $LiNi_{0.5}Mn_{1.5}O_4$ allows the fast diffusion of lithium and can improve the rate performance because of its three-dimensional interstitial space. Meanwhile, the layered phase of $Li[Li_xM_{1-x}]O_2$ provides high specific capacity. When synthetized at temperatures of 900, 1000 and 1100 °C, capacities of 276, 262 and 250 mA h g^{-1} were obtained, respectively (60^{th} cycle at 0.1 C), showing higher values compared to spinel compounds and comparable to layered compounds (Huang et al. 2018).

The olivine crystal used on positive electrodes is recognized for their high thermal stability and high capacity. Most olivines contain Fe, Mn and Co: $LiFePO_4$; $LiMnPO_4$ and $LiCoPO_4$ with theoretical specific capacities of 170, 171 and 167 mA h g^{-1}, respectively. In $LiFePO_4$, Li^+ and Fe^{2+} ions are located in octahedral sites whereas P is in tetrahedral sites. This compound has relatively low intercalation voltage and poor ionic conductivity. $LiMnPO_4$ offers 0.4 V higher intercalation voltage compared to olivine with Fe, leading to higher specific energy, but with lower ionic conductivity. Recently, El Khalfaouy et al. (2019) have developed a new compound using yttrium-substituted phospho-olivine in different proportions $LiMn_{1-x}Y_xPO_4/C$. When x = 0.01, the material shows an excellent capacity and stability during charge/discharge processes. The initial specific discharge capacity can reach up to 156.84 mA h g^{-1} at C/20, with a coulombic efficiency of about 96.11%, which is 14% higher than that of the non-doped material. The authors suggest that yttrium has been incorporated into the host material structure, enhancing the electronic conductivity and improving lithium ion mobility inside the structure.

Polyanionic compounds were proposed in order to improve the ionic conductivity, compared to olivine compounds. These materials have tavorite structures of the type $LiMPO_4(OH)_xF_{1-x}$ (M = Al, Ga, V, Fe, Mn, and Ti) where some M^{3+} compounds are abundant in the earth's crust (Fe^{3+} and Al^{3+}) (Ramesh et al. 2010). The fluorophosphates tavorites $LiVPO_4F$, Li_2CoPO_4F and Li_2NiPO_4F are good positive electrodes in Li-ion batteries with specific discharge capacity around 150 mA h g^{-1}. Other compounds of the polyanionic class are the oxyphosphates $LiVOPO_4$ (110 mA h g^{-1}) and fluorosulfates $LiFeSO_4F$, $LiCoSO_4F$ and $LiNiSO_4F$ with specific discharge capacities around 130 mA h g^{-1} (Li et al. 2017b).

Both the electrochemical mechanism and the component constitution of SIB and LIB are very similar, except for their charge carries, which involves an interstitial intercalation of a guest species into a host material. As for the positive electrodes specific challenges must be considered: sodium has a less negative reduction potential when compared to lithium (-2.71 V vs SHE and -3.02 V vs SHE, respectively) which affects its maximum energy density; another point is that sodium ions are bigger than lithium (ionic radius 1.02 Å and 0.76 Å, respectively) which creates incompatibility with some traditional intercalation materials (Hwang et al. 2017).

In SIBs, the positive electrode consists of a material that can reversibly perform Na^+ intercalation/de-intercalation reactions at a voltage considered reasonably greater than 2 V (vs. Na/Na^+). While these electrodes work as a host matrix for Na^+, the change in volume should be as minimal as possible during the Na^+ intercalation/(de)intercalation cycles, and this ability is critical for long-term battery cycling performance (Slater et al. 2013). During the last years, many different materials have been studied for SIBs positive electrode, including layered transition metal oxides, tunnel type oxide structures, sulfate and phosphate based polyanionic compounds (Sun et al. 2019).

Layered transition metal oxides are structures composed by alternating layers of alkali ion and transition metal (TM)-ion, and for the sodium case they are usually referred as Na_xTMO_2. Due to the large size of the Na ion, when compared to Li ion, some differences in the structures are noticed. For instance, the anion framework could either be a close-packed or non-close-packed, while for Li it is usually close-packed. When the sodium ion occupies octahedral interstitial sites in the layered Na_xTMO_2 it is said to have an O-type stacking sequence; when it occupies trigonal-prismatic interstitial sites it has a P-type stacking sequence (Sun et al. 2019). The first studies on the electrochemical behavior of Na-ion intercalation in layered transition-metal oxides were published by Mendiboure et al. (1985), early in the 1980s. Among the most interesting aspects of these compounds one can find high theoretical capacities, suitable working voltages and a diversity of synthetic routes (Chen et al. 2019).

Layered manganese oxides, Na_xMnO_2, are materials that have the flexibility of forming structures with either O- or P-type stacking sequences depending on the concentration of sodium, besides presenting the advantages of low cost and earth abundance. A layered $NaMn_3O_5$ material with a Birnessite structure was synthesized by a simple route consisting of a redox reaction followed by a hydrothermal treatment was reported by Guo et al. (2014). The obtained $NaMn_3O_5$ positive electrode showed a high capacity of 219 mA h g^{-1} (72.5% of its theoretical capacity), and exhibited a good rate capability of 115 mA h g^{-1} at a 5 C rate.

For the cases where Na_xTMO_2 contains several stacking sequences, it is usual for the P-type phases to have an insufficient amount of

sodium, i.e. $x < 1$, while the oxides with O-type phase usually shows an amount of sodium close to the sufficient, i.e. $x \sim 1$. This means that the O-type phase has a superior specific capacity, since it can have more sodium extracted from its structure than the P-type. However, the structural configuration of two adjacent face sharing sites in the trigonal prismatic structure found in the P-type lattice facilitates the diffusion of sodium ions, which means a better performance of rate capability for P-type based electrodes over O-type (Sun et al. 2019). A P2/O3 biphasic material, $Na_{0.67}Ni_{0.33}Mn_{0.57}Sn_{0.1}O_2$ was synthesized and used as a positive material for SIBs, providing an initial capacity of 155 mA h g^{-1} at 15 mA g^{-1}, with good rate and cycling performance. This electrochemical response was attributed to the mixture of the two phases which promoted a synergistic effect (Li et al. 2019a).

Some transition metal oxides studied as positive electrodes for SIBs have a especial arrangement with connected octahedral and square-pyramidal sites, which forms a tunnel shaped lattice that can promote rapid sodium ion diffusion and consequently superior storage performance (Yabuuchi et al. 2014). This is the case of single crystalline $Na_{0.44}MnO_2$ nanowires synthesized by Cao et al. (2011) using a polymer-pyrolysis method. When applied as SIBs electrodes, it produced a capacity of 128 mA h g^{-1} at 0.1 C, with 77% capacity retention after 1000 cycles at 0.5 C.

Doping tunnel structured oxides with fluorine is an interesting option to enlarge the tunnel lattices and to facilitate the mobility of the sodium ions, since ions containing fluorine have higher electronegativity and smaller ionic radius in comparison to ions containing oxygen. A series of F-doped $Na_{0.66}Mn_{0.66}Ti_{0.34}O_{2-x}F_x$ were synthesized and studied by Wang et al. (2018); diffusion coefficient of the sodium ions confirmed the enlargement of the tunnels, which resulted in a good rate performance of the electrodes. The highest obtained capacity was 97 mA h g^{-1} at 0.2 C, and the electrode provided 85 mA h g^{-1} at 2 C for 1000 cycles.

The presence of polyanion groups, e.g. phosphates and fluorophosphates, in transition metal oxides increases the electrode operating voltage (vs Na/Na^+) due to inductive effect promoted by these groups. This interesting characteristic can be explored in order to improve the SIBs energy density (Yabuuchi et al. 2014). $Na_3V_2(PO_4)_3$ is a very promising electrode material due to its Na super ionic conductor (NASICON) structure, theoretical capacity (117.6 mA h g^{-1}) and flat potential plateaus around 3.4 V (vs Na/Na^+). However, it has poor conductivity that leads to a limited rate capability. In order to avoid the conductivity hindrance, Huang et al. (2019) synthesized and studied a carbon coated $Na_3V_2(PO_4)_3$ composite doped with nitrogen through a sol-gel process followed by sintering. The presence of a nitrogen-doped carbon layer helped obtaining high sodium diffusion coefficients by shortened diffusion lengths, and improving the electronic conductivity. The prepared electrode exhibited capacities of 109.2 mA h g^{-1} at 0.2 C and 87.2 mA h g^{-1} at 20 C, with a capacity retention of 91.2% after 500 at 2 C.

Sodium vanadium fluorophosphate family materials, $Na_3V_2(PO_4)_2O_{2x}F_{3-2x}$ ($0 \leq x \leq 1$), combine the electronegativity of the PO_4^{3-} groups with F^- ions. The result is electrodes with operating voltages close to 4.0 V (vs Na/Na^+), nevertheless its theoretical capacity is close to 130 mA h g^{-1}, depending on V oxide state. Xu et al. (2019a) developed a hydrothermal method to synthesize carbon coated $Na_3V_2(PO_4)_2O_2F$ nanoparticles and studied their electrochemical properties. The small particle size coupled with electronic conductivity enhancement from the carbon layers helped the electrode to provide a capacity of 121.5 mA h g^{-1}, at 1 C (3 - 4.5 V vs Na/Na^+).

Transformation

Positive conversion electrodes are being widely studied as potentially high-energy-density alternatives to intercalation-based materials to increase specific capacity and enable effective application in batteries (Grimaud et al. 2016). Moreover, these compounds are capable of storing between 2 and 3 Li per atom (Grimaud 2017, Wu & Yushin 2017). LIBs have two types of reactions, shown in equations 5 and 6:

Type 1: $M^{+}X_z + yLi \rightleftharpoons M + zLi_{(y/z)}X$ (5)

Type 2: $yLi + X^{-} \rightleftharpoons Li_yX$ (6)

Where, M^{+} can be Fe^{3+}, Fe^{2+}, Ni^{2+}, Cu^{2+}, Mn^{3+}, M is the reduced material, and X^{-} can be F^{-}, Cl^{-}, Br^{-}, I^{-}, S^{2-}, Se^{2-}.

In general, the most commonly used substances for this type of electrode are some of the most abundant and environmentally friendly materials such as O, S, Fe, and Cu. As mentioned, two types of reactions can occur: type 1, with true conversion, and type 2, chemical transformation.

For a type 1 reaction, in general the reduction of metal halides to the elemental form of the metal requires more than one lithium, which leads to theoretical capacities ranging from 500 to 800 mA h g^{-1} to CoF_3, CuF_2, NiF_2, FeF_3, FeF_2, VF_3. This conversion reaction transforms a single phase ($M^{+}X_z$) in two phases (LiX and M).

For type 2, the reaction is a chemical transformation of a single phase in another single phase. During the charge/discharge process there is an alternation between the phases with the elemental material (X^{-}) and the lithium aggregate state (Li_yX). Recently, chalcogen and chalcogenide materials including Se e Li_2Se (Liu et al. 2016b, Song et al. 2019a), Te e Li_2Te, and S and Li_2S (Meini et al. 2014, Wild et al. 2015) have received considerable attention as promising positive electrode candidates for next-generation rechargeable lithium-ion and lithium batteries. Both reaction types are exemplified in Figure 5 and specific capacity and operating voltage are shown in Figure 6.

Lithium sulfur batteries will be highlighted in the review due to their higher specific theoretical capacity compared to LIBs. The electrolytes for Li–S battery system are usually ether-based solvents such as 1,3-dioxolane (DOL), 1,2-dimethoxyethane (DME), and tetra-(ethylene glycol) dimethyl ether (TEGDME), since carbonate-based electrolytes react with polysulfides irreversibly.

In addition to being low cost, recovered from industrial waste, nontoxic and abundant, sulfur has a theoretical capacity approximately 5 times higher than transition metal oxides and phosphates, and it has an energy density of 2600 W h kg^{-1}. These are the main facts that favor the large scale application of sulfur (Ma et al. 2017b, Tao et al. 2016, Worthington et al. 2017).

Electrochemical reduction of sulfur at the positive electrode produces low oxidation state polysulfides according to the following equations (7 to 11). Two plateaus are clearly defined in a typical discharge profile when used in a cell with liquid electrolytes (Medenbach & Adelhelm 2017, Talaie et al. 2017).

Soluble	$2e^{-} + 2\,Li^{+} + S_8 \rightleftharpoons Li_2S_8$	(7)
	$2e^{-} + 2\,Li^{+} + 3\,Li_2S_8 \rightleftharpoons 4\,Li_2S_6$	(8)
	$2e^{-} + 2\,Li^{+} + 2\,Li_2S_6 \rightleftharpoons 3\,Li_2S_4$	(9)
Insoluble	$2e^{-} + 2\,Li^{+} + Li_2S_4 \rightleftharpoons 2\,Li_2S_2$	(10)
	$2e^{-} + 2\,Li^{+} + Li_2S_2 \rightleftharpoons 2\,Li_2S$	(11)

However, several problems of capacity loss and low coulombic efficiency have yet to be overcome (Hong et al. 2018, Wang et al. 2015c):

(i) The insulating effect of sulfur reduces electrical conductivity, which causes electrochemically slow reactions;

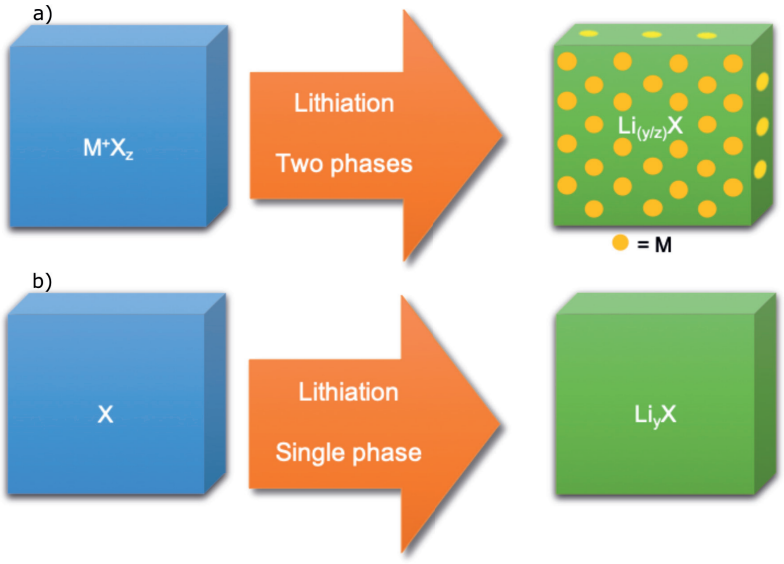

Figure 5. (a) Conversion type 1 with formation of two phases and (b) conversion type 2 with transformation of a single-to-single phase.

(ii) The long chain polysulphides formed during the discharge process are soluble in the electrolyte and permeate through the separator, resulting in a shuttle effect that leads to charge deficiency and rapid loss of capacity (by mass loss);

(iii) Large volumetric expansion (80%) after discharge occurs with the complete transformation of sulfur into Li_2S, which may lead to electrode spraying.

Numerous attempts have been made to overcome these challenges, such as optimization of the positive electrode structure, nanostructuring of active materials, including additives to electrolyte and/or electrode, and modifying the polymer separator. Some of the widely explored materials to increase the electrode conductivity and provide physical confinement/entrapment of lithium polysulfides are micro-nanostructured sulfur encapsulate materials, nano conductive and porous carbon materials such as: carbon nanotubes, carbon nanowires, porous carbon, graphene, carbon fibers, as well as compounds such as conductive polymers and porous silica (Chen et al. 2013, Lyu et al. 2015, Shao et al. 2013, Wang et al. 2013). Recently, Metal-Organic Frameworks (MOFs) have been studied to encapsulate sulfur (Hong et al. 2018, Zhao et al. 2016, Zhou et al. 2014, 2015). MOFs are crystalline materials composed of metal ion junctions and organic ligands in infinite matrices, diverse geometries, and possess great synthetic versatility (Cui et al. 2012). ZIF8 (Zeolitic Imidazolate Framework-8) is a well-studied MOF that plays a very promising role, because it is electrochemically inert and stable. Some authors have reported specific capacities around 1000 mA h g^{-1} at 0.1 C (Zhou et al. 2014).

Na-S batteries are usually constituted of molten sodium and sulfur as negative and positive electrodes, respectively, and β-alumina as a sodium conducting ceramic electrolyte. They were first proposed by the Ford Company in the 1970's and since then have been studied aiming stationary applications. Among the attractive characteristics of these cells one can find an interesting theoretical specific energy of 760 W h kg^{-1}, low self-discharge rate, temperature stability, low-cost of the components, and safety due to solid electrolyte. The big hindrance of this type of cell is that part of the produced energy is used to maintain their high operating temperatures (300-350 °C), which reduces the

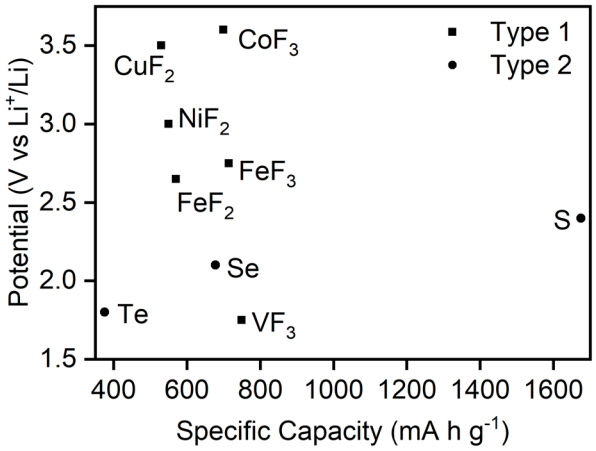

Figure 6. Theoretical specific capacity of conversion positive materials. CoF_3, CuF_2, NiF_2, FeF_3, FeF_2, and VF_3 (Wu & Yushin 2017); Se and Li_2Se (Liu et al. 2016b, Song et al. 2019a); Te and Li_2Te (Koketsu et al. 2016); S and Li_2S (Meini et al. 2014, Wild et al. 2015, Zhou et al. 2014).

efficiency of the system. The overall charge/discharge reaction can be seen in the equation 12, which gives an electromotive force of 2.08 V (Hueso et al. 2013).

$$2Na + xS \underset{\text{charge}}{\overset{\text{discharge}}{\rightleftarrows}} Na_2S_x \quad (12)$$

The elemental sulfur used as positive electrode in Na-S batteries has a high theoretical specific capacity of 1675 mA h g^{-1}, considering a two-electron reaction as shown in the equation 13. However, due to the formation of electrical insulator by-products during the discharge process, i.e. polysulphides, the value cannot be reached and the active species performance is limited by the gravimetric capacity of 836 mA h g^{-1} (Hueso et al. 2013, Lu et al. 2010).

$$xS + 2e^- \underset{\text{charge}}{\overset{\text{discharge}}{\rightleftarrows}} S_x^{2-} \quad (13)$$

Molten sulfur and polysulphide compounds are highly corrosive, which implies in the use of protective steel layers and constitute a challenge in the search for a current collector. An extremely vigorous reaction between sodium and sulfur might occur if there is any rupture in the β-alumina membrane, which can result in fire and explosion (Hueso et al. 2013, Lu et al. 2010).

The use of a transition metal chloride as the positive electrode, along with a secondary molten electrolyte of $NaAlCl_4$ (melting point, 170 °C), can assure some operational advantages over traditional Na-S battery such as higher theoretical energy density (788 W h kg^{-1}) and operating voltage, as well as better tolerance against overcharging. In these cells, the molten electrolyte works as a Na transport medium between the β-alumina and the positive electrode. It also makes the system safer due to the less vigorous reaction with molten sodium, in case of broke β-alumina (Hueso et al. 2013, Lu et al. 2010).

The positive electrode, which must be insoluble in the molten electrolyte, is usually a porous structure of nickel chloride impregnated with $NaAlCl_4$ salt. The addition of iron to the cell increases the power response. Equation 14 shows the charge/discharge reactions of the nickel configuration, which provides an electromotive force of 2.58 V, while the charge/discharge reactions of the iron configuration can be seen in the equation 15, which generates an electromotive force of 2.35 V (Hueso et al. 2013, Lu et al. 2010).

$$NiCl_2 + 2Na \underset{\text{charge}}{\overset{\text{discharge}}{\rightleftarrows}} Ni + 2NaCl \quad (14)$$

$$FeCl_2 + 2Na \underset{\text{charge}}{\overset{\text{discharge}}{\rightleftarrows}} Fe + 2NaCl \quad (15)$$

Both safety and electrochemical issues concerning high temperature Na-S batteries have led to the search for room temperature

systems. Nevertheless, these batteries have some other challenges such as low sulfur utilization and dissolution of polysulfide intermediates which can cause a "shuttle" of the negative sulfur electrode. Microporous carbon has been found suitable for both to improve electric conductivity and to provide good confinement/immobilization for sulfur and its reduced products (Wei et al. 2016). Kumar et al. (2019) obtained a high energy density room temperature Na-S battery by incorporating MnO_2 nanoneedle arrays on a flexible carbon cloth substrate containing Na_2S_6, which worked as a multifunctional positive electrode and provided an initial energy density of 946 W h kg^{-1}, dropping to 728 W h kg^{-1} after 500 cycles.

Metal-Air batteries can also be highlighted due to their high specific capacity, and approaching the energy density of gasoline when Li is used as negative electrode. This kind of battery can be based on aqueous or non-aqueous electrolytes, and both of them rely on the electrochemistry of O_2 at the positive electrode. The electrolyte will play a major role on the products formed during battery discharge. While the reduction of O_2 in aqueous electrolyte involves O-O bond cleavage, forming OH^-, the reaction in non-aqueous electrolytes forms peroxide, and there is no bond cleavage (Bruce et al. 2012).

As mentioned in a previous section, the negative electrode of a metal-air battery is either lithium or sodium, for Li-Air or Na-Air batteries, respectively. On the other hand, the positive electrode is composed of a material that allows the oxygen reaction to occur reversibly. Carbon is widely used for this matter. It is the oxygen electrochemical reaction at the positive electrode where lies one of the major problems on metal-air batteries. The pathway for the redox reactions is not the same, which generates a hysteresis between charge and discharge plateaus (Figure 7), causing a low energy efficiency. On top of that, carbon can also go through corrosion when cell is charged to voltages higher than 3.5 V (McCloskey et al. 2012). Li_2O_2 formed during discharge is electronic insulating and the particles can block the carbon pores, lowering coulombic efficiency. To overcome those problems, redox mediators have been proposed, in way to favour the formation of Li_2O_2 in solution and not at the electrode surface. These redox mediators are solubilized in the electrolyte and can act in different ways, as through redox-shuttle or complex intermediate. Viologens and benzoquinones are examples of redox mediators that favour the Li_2O_2 formation through the solution mechanism (Aetukuri et al. 2015, Lim et al. 2016, Liu et al. 2018).

Electrolytes

In general, the electrolyte of a metal ion battery must be a solvent stable enough through the faradaic reactions (as discussed previously), and have a metal ion salt in high concentration. The transport number of the metal ion must be as

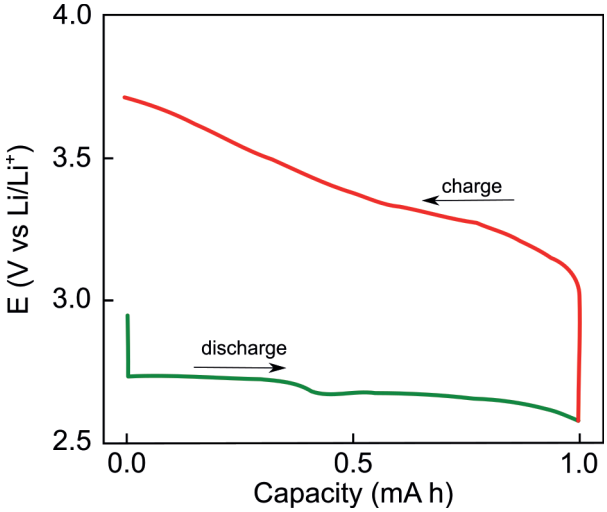

Figure 7. Discharge (green line) and charge (red line) of a Li-O_2 battery with a carbon positive electrode and dimethyl ether with 0.25 mol L^{-1} of $LiTf_2N$ and 0.2 mol L^{-1} of LiI as electrolyte. Adapted from (Burke et al. 2016), with permission from the American Chemical Society.

high as possible. However, the chemistry at each of the different electrodes may require certain specificity on the electrolyte. Nowadays, the state-of-the-art electrolyte for Li-ion battery is composed of a mixture of carbonate solvents, as ethylene carbonate and dimethyl carbonate (50:50 v/v), with 1.0 mol L^{-1} of $LiPF_6$, and proportions can vary (Guyomard & Tarascon 1995). The electrolyte also plays an important role on the formation of the SEI on early cycles, and PF_6^- anions are involved on the mechanism (typically forming LiF). Additives can also be added to the electrolyte to assist on the formation of such layer, including the CEI. Most common additives are vinylene carbonate and vinyl ethylene carbonate, but many others are also used (Zhang 2006). Different anions can be used for the electrolyte preparation, and most of them present fluorine in its formulation, for the SEI formation. $LiTf_2N$ (bis(trifluoromethylsulfonyl) imide anion), LiFSI, $LiBF_4$, and $LiCF_3SO_3$ are a few examples in this category. The same anions can also be used for the preparation of Na-ion battery electrolytes.

In order to increase the battery operating voltage, electrolytes with higher electrochemical stability towards oxidations is necessary. For instance, Zhang et al. (2013) showed that through fluorination of organic carbonates, stability up to 5 V can be achieved. Another alternative to increase electrochemical stability is the development of ionic liquid-based electrolyte. Elia et al. (2016) used Tf_2N- and FSI-based ionic liquids in Li-ion batteries and showed that extended cycle life could be achieved. Moreover, they observed that the rate capability was improved when electrolyte contained FSI ionic liquid. Ionic liquid electrolytes also show high thermal stability, and a large variety of chemical functionalization is possible, which can play important role on battery operation (Galiote et al. 2017), however, one must take in account any incompatibility between chemical groups in the ionic liquids with the cell components. For instance, imidazolium cations can show an acid hydrogen in the five-member cycle, which can react with lithium. The substitution of these hydrogens with a methyl group remove the reactivity with metal, making it a more compatible electrolyte (Bazito et al. 2007, Wang et al. 2007).

Solid electrolytes were proposed to increase safety and remove the possibility of electrolyte leakage if a cell is compromised. They have been studied since the 1970s, especially using poly(ethylene) oxide (PEO) (Armand 1994, Xue et al. 2015), but no formulation has reached the market yet. The major problem that hampers their application is the low ionic conductivity when compared with their liquid counterparts. Many progresses have been made nowadays in gel electrolytes, for instance using polymers and ionic liquids, or even poly(ionic liquids) (MacFarlane et al. 2016, Torresi et al. 2018).

More recently, high voltage aqueous LIBs were proposed using highly concentrated aqueous electrolyte. Suo et al. (2015) showed that a solution of 21 molal of $LiTf_2N$ in water completely changes the interactions between water molecules and Li^+. The stronger interaction due to low availability of water expands the electrolyte stability (Martins & Torresi 2020). Since then, cells containing highly concentrated aqueous electrolytes (also called water-in-salt electrolyte, WiSE) were shown to be stable for batteries using different positive electrodes (Suo et al. 2016, Wang et al. 2016, Yang et al. 2019a) and even Li-O_2 (Dong et al. 2018) and Sulfur batteries (Yang et al. 2017a). Dubouis et al. (2018) showed that water reduction at the negative electrode and so the production of hydroxyl groups was responsible for the production of LiF and the formation of SEI, and not the direct reduction of the anions Tf_2N^- as previously proposed.

FUTURE PERSPECTIVES

The Nobel prize in Chemistry was awarded in 2019 to Goodenough, Whittingham and Yoshino for the development of the Li-ion battery. Their findings paved the way for the electric revolution in which we live today. From devices that enabled information access nearly everywhere to electric vehicles, they are all powered by an electrochemical energy storage device like a lithium-ion battery. The significant increase in the demand for electrochemical energy storage devices escalated the search for new materials. Many strategies have been used to find cheaper electroactive materials in morphologies that can favor a better performance and also more efficient redox reactions; that is, new research and development projects are underway where enormous efforts are being made to increase the quantity (energy stored by mass or volume of the device) and the operation speed (power to store and extract energy). The major driving force to achieve these objectives are related to the synthesis of new materials for the electrodes (with strong indication that nanostructure can enhance performance) where the kinetics of the redox reaction is faster (current increase) and the quantity of electrons that can be stored is greater (energy). In this regard, it is also important to increase the operation of the devices (greater potential where the redox reaction occurs (for batteries) or greater electrolyte/electrode stability (for electrochemical capacitors)). Therefore, it is important to develop new electrolytes that are electrochemically stable in the potentials where the electrodes undergo to the redox reaction; an example, it is the development of ionic liquids. In this case, in addition to its electrochemical stability, its thermal stability makes them suitable for use in safer devices. The safety of electrochemical energy storage devices is a key point as they are all high energy density devices. Avoiding chemical decomposition that can lead to flammable products is a non-negotiable requirement for stationary (for example, smart electricity distribution networks) and non-stationary (electric vehicles) applications. Finally, considering the availability of chemicals to synthesize different materials, it is possible to assume that in the future there will be a coexistence of different technologies for electrochemical energy storage, where the type of application will contribute to the definition of what type of storage will be more efficient for each application.

List of Acronyms

HOMO: highest occupied molecular orbital
LUMO: lowest unoccupied molecular orbital
SEI: solid electrolyte interphase
CEI: cathode electrolyte interphase
SHE: standard hydrogen electrode
SIB: sodium-ion battery
LIB: lithium-ion battery
SLG: single-layer graphene
FLG: few-layers graphene
LTO: lithium titanate
NTO: sodium trititanate
TMOs: transition metal oxides
C NPs: Carbon coated nanoparticles
G2: Graphite Micrograf
N-G: nitrogen-doped graphene
GNRs: Graphene nanoribbons
GN: Graphene nanocomposites
ICE: initial coulombic efficiency
TEOS: tetraethoxysilane
TTCS: 1,3,5,7-tetramethyl-1,3,5,7-tetravinylcyclotetrasiloxane
GNPs: graphene nanoplatelets
FSI^-: bis(fluorosulfonyl)imide anion
LCO: lithium cobalt oxide
LNO: lithium nickel oxide

NMC (or NCM): lithium nickel manganese cobalt oxide – metals can show different stochiometric proportions
NCA: lithium nickel cobalt aluminium oxide
LMO: lithium manganese oxide
TM: transition metal
NASICON: sodium super ionic conductor
DOL: 1,3-dioxolane
DME: 1,2-dimethoxyethane
TEGDME: tetra-(ethylene glycol) dimethyl ether
MOF: metal-organic framework
ZIF8: zeolitic imidazolate framework-8
Tf_2N^-: bis(trifluoromethylsulfonyl) imide anion
PEO: poly(ethylene) oxide
WiSE: water-in-salt electrolyte

Acknowledgments

This work was supported by the Conselho Nacional de Desenvolvimento Científico e Tecnológico (CNPq, 303141/2017-4), Coordenação de Aperfeiçoamento de Pessoal de Nível Superior (CAPES) and Fundação de Amparo à Pesquisa do Estado de S. Paulo (FAPESP, 2015/26308-7). VLM (13/22748-7), IEM (17/20043-7), MML (19/02669-1), PFMO (17/15456-0), RMA (17/15469-5), SC (18/11320-0), WGM (18/23072-0), TTO (17/10046-9) and BLS (19/09341-1) wish to thank FAPESP for scholarships. ECM (88882.328255/2019-01) thanks CAPES for scholarship.

REFERENCES

AETUKURI NB, MCCLOSKEY BD, GARCÍA JM, KRUPP LE, VISWANATHAN V & LUNTZ AC. 2015. Solvating additives drive solution-mediated electrochemistry and enhance toroid growth in non-aqueous Li–O2 batteries. Nat Chem 7: 50-56.

ANDERSEN HF, FOSS CEL, VOJE J, TRONSTAD R, MOKKELBOST T, VULLUM PE, ULVESTAD A, KIRKENGEN M & MÆHLEN JP. 2019. Silicon-Carbon composite anodes from industrial battery grade silicon. Sci Rep 9: 14814.

ANDERSSON S & WADSLEY AD. 2002. The crystal structure of Na2Ti3O7. Acta Crystallogr 14: 1245-1249.

ANJI REDDY M, HELEN M, GROSS A, FICHTNER M & EUCHNER H. 2018. Insight into Sodium Insertion and the Storage Mechanism in Hard Carbon. ACS Energy Lett 3: 2851-2857.

ANWER S, HUANG Y, LIU J, LIU J, XU M, WANG Z, CHEN R, ZHANG J & WU F. 2017. Nature-Inspired Na2Ti3O7 Nanosheets-Formed Three-Dimensional Microflowers Architecture as a High-Performance Anode Material for Rechargeable Sodium-Ion Batteries. ACS Appl Mater Interfaces 9: 11669-11677.

ARMAND M. 1994. The history of polymer electrolytes. Solid State Ionics 69: 309-319.

ARMSTRONG AR & BRUCE PG. 1996. Synthesis of layered LiMnO2 as an electrode for rechargeable lithium batteries. Nature 381: 499-500.

ASSRESAHEGN BD & BÉLANGER D. 2017. Synthesis of binder-like molecules covalently linked to silicon nanoparticles and application as anode material for lithium-ion batteries without the use of electrolyte additives. J Power Sources 345: 190-201.

BAK SM ET AL. 2014. Structural Changes and Thermal Stability of Charged LiNi x Mn y Co z O 2 Cathode Materials Studied by Combined In Situ Time-Resolved XRD and Mass Spectroscopy. ACS Appl Mater Interfaces 6: 22594-22601.

BALDINELLI A, DOU X, BUCHHOLZ D, MARINARO M, PASSERINI S & BARELLI L. 2018. Addressing the energy sustainability of biowaste-derived hard carbon materials for battery electrodes. Green Chem 20: 1527-1537.

BAZITO FFC, KAWANO Y & TORRESI RM. 2007. Synthesis and characterization of two ionic liquids with emphasis on their chemical stability towards metallic lithium. Electrochim Acta 52: 6427-6437.

BLOMGREN GE. 2017. The Development and Future of Lithium Ion Batteries. J Electrochem Soc 164: 5019-5025.

BRACAMONTE MV, PRIMO EN, LUQUE GL, VENOSTA L, BERCOFF PG & BARRACO DE. 2017. Lithium dual uptake anode materials: crystalline Fe3O4 nanoparticles supported over graphite for lithium-ion batteries. Electrochim Acta 258: 192-199.

BRUCE PG, FREUNBERGER SA, HARDWICK LJ & TARASCON JM. 2012. Li-O2 and Li-S batteries with high energy storage. Nat Mater 11: 19-29.

BRUCE PG, ARMSTRONG AR & GITZENDANNER RL. 1999. New intercalation compounds for lithium batteries: layered LiMnO2. J Mater Chem 9: 193-198.

BURKE CM, BLACK R, KOCHETKOV IR, GIORDANI V, ADDISON D, NAZAR LF & MCCLOSKEY BD. 2016. Implications of 4 e - Oxygen Reduction via Iodide Redox Mediation in Li-O2 Batteries. ACS Energy Lett 1: 747-756.

CAO Y, XIAO L, WANG W, CHOI D, NIE Z, YU J, SARAF LV, YANG Z & LIU J. 2011. Reversible Sodium Ion Insertion in Single Crystalline Manganese Oxide Nanowires with Long Cycle Life. Adv Mater 23: 3155-3160.

CHAUQUE S, OLIVA FY, VISINTIN A, BARRACO D, LEIVA EPM & CÁMARA OR. 2017. Lithium titanate as anode material for lithium ion batteries: Synthesis post-treatment and its electrochemical response. J Electroanal Chem 799: 142-155.

CHAUQUE S, BRAGA AH, GONÇALVES RV, ROSSI LM & TORRESI RM. 2020. Enhanced energy storage of Fe3O4 nanoparticles embedded in N-doped graphene. ChemElectroChem 7: 1456-1464.

CHEN K, YANG H, LIANG F & XUE D. 2018. Microwave-Irradiation-Assisted Combustion toward Modified Graphite as Lithium Ion Battery Anode. ACS Appl Mater Interfaces 10: 909-914.

CHEN M, CHOU S & DOU SX. 2019. Understanding Challenges of Cathode Materials for Sodium-Ion Batteries using Synchrotron-Based X-Ray Absorption Spectroscopy. Batter Supercaps 2: 842-851.

CHEN R, ZHAO T, LU J, WU F, LI L, CHEN J, TAN G, YE Y & AMINE K. 2013. Graphene-Based Three-Dimensional Hierarchical Sandwich-type Architecture for High-Performance Li/S Batteries. Nano Lett 13: 4642-4649.

CHEN T, WU J, ZHANG Q & SU X. 2017. Recent advancement of SiOxbased anodes for lithium-ion batteries. J Power Sources 363: 126-144.

CHO J, KIM YW, KIM B, LEE JG & PARK B. 2003. A Breakthrough in the Safety of Lithium Secondary Batteries by Coating the Cathode Material with AlPO4 Nanoparticles. Angew Chemie Int Ed 42: 1618-1621.

CHOI S & MANTHIRAM A. 2002. Synthesis and Electrochemical Properties of LiCo2O4 Spinel Cathodes. J Electrochem Soc 149: A162.

CUI Y, YUE Y, QIAN G & CHEN B. 2012. Luminescent Functional Metal-Organic Frameworks. Chem Rev 112: 1126-1162.

DAHN JR, XING W & GAO Y. 1997. The "falling cards model" for the structure of microporous carbons. Carbon 35: 825-830.

DAMODAR D, GHOSH S, USHA RANI M, MARTHA SK & DESHPANDE AS. 2019. Hard carbon derived from sepals of Palmyra palm fruit calyx as an anode for sodium-ion batteries. J Power Sources 438: 227008.

DARWICHE A, MARINO C, SOUGRATI MT, FRAISSE B, STIEVANO L & MONCONDUIT L. 2012. Better cycling performances of bulk sb in na-ion batteries compared to li-ion systems: An unexpected electrochemical mechanism. J Am Chem Soc 134: 20805-20811.

DAVID L, BHANDAVAT R, BARRERA U & SINGH G. 2016. Silicon oxycarbide glass-graphene composite paper electrode for long-cycle lithium-ion batteries. Nat Commun 7: 10998.

DENG X, CHEN Z & CAO Y. 2018. Transition metal oxides based on conversion reaction for sodium-ion battery anodes. Mater Today Chem 9: 114-132.

DONG Q, YAO X, ZHAO Y, QI M, ZHANG X, SUN H, HE Y & WANG D. 2018. Cathodically Stable Li-O2 Battery Operations Using Water-in-Salt Electrolyte. Chem 4: 1345-1358.

DOU X, GENG C, BUCHHOLZ D & PASSERINI S. 2018. Research Update: Hard carbon with closed pores from pectin-free apple pomace waste for Na-ion batteries. Apl Mater 6: 047501.

DOU X, HASA I, HEKMATFAR M, DIEMANT T, BEHM RJ, BUCHHOLZ D & PASSERINI S. 2017. Pectin Hemicellulose or Lignin? Impact of the Biowaste Source on the Performance of Hard Carbons for Sodium-Ion Batteries. ChemSusChem 10: 2668-2676.

DOU X, HASA I, SAUREL D, VAALMA C, WU L, BUCHHOLZ D, BRESSER D, KOMABA S & PASSERINI S. 2019. Hard carbons for sodium-ion batteries: Structure analysis sustainability and electrochemistry. Mater Today 23: 87-104.

DUBOUIS N, LEMAIRE P, MIRVAUX B, SALAGER E, DESCHAMPS M & GRIMAUD A. 2018. The role of the hydrogen evolution reaction in the solid-electrolyte interphase formation mechanism for " Water-in-Salt " electrolytes. Energy Environ Sci 11: 3491-3499.

ELIA GA, ULISSI U, JEONG S, PASSERINI S & HASSOUN J. 2016. Exceptional long-life performance of lithium-ion batteries using ionic liquid-based electrolytes. Energy Environ Sci 9: 3210-3220.

EL KHALFAOUY R, TURAN S, RODRIGUEZ MA, DERMENCI KB, SAVACI U, ADDAOU A, LAAJEB A & LAHSINI A. 2019. Solution combustion synthesis and electrochemical properties of yttrium-doped LiMnPO4/C cathode materials for lithium ion batteries. J Rare Earths 1: 1173-1178.

GALIOTE NA, JEONG S, MORAIS WG, PASSERINI S & HUGUENIN F. 2017. The Role of Ionic Liquid in Oxygen Reduction Reaction for Lithium-air Batteries. Electrochim Acta 247: 610-616.

GAO H, XIN S, XUE L & GOODENOUGH JB. 2018. Stabilizing a High-Energy-Density Rechargeable Sodium Battery with a Solid Electrolyte. Chem 4: 833-844.

GE T, GUO Z, WU M, SUN R, LI W & YANG G. 2019. Preparation and characterization of spinel-layered mixed structural 0.2LiNi0.5Mn1.5O4·0.8Li[Li0.2Ni0.2Mn0.6]O2 as cathode materials for lithium-ion batteries. J Alloys Compd 801: 254-261.

GOKTAS M, AKDUMAN B, HUANG P, BALDUCCI A & ADELHELM P. 2018. Temperature-Induced Activation of Graphite Co-intercalation Reactions for Glymes and Crown Ethers in Sodium-Ion Batteries. J Phys Chem C 122: 26816-26824.

GOMEZ-MARTIN A, MARTINEZ-FERNANDEZ J, RUTTERT M, WINTER M, PLACKE T & RAMIREZ-RICO J. 2019. Correlation of Structure and Performance of Hard Carbons as Anodes for Sodium Ion Batteries. Chem Mater 31: 7288-7299.

GOODENOUGH JB. 2013. Evolution of Strategies for Modern Rechargeable Batteries. Acc Chem Res 46: 1053-1061.

GRIMAUD A. 2017. Batteries: Beyond intercalation and conversion. Nat Energy 2: 17003.

GRIMAUD A, HONG WT, SHAO-HORN Y & TARASCON JM. 2016. Anionic redox processes for electrochemical devices. Nat Mater 15: 121-126.

GU J, WU J, GU D, ZHANG M & SHI L. 2012. All-Digital Wide Range Precharge Logic 50% Duty Cycle Corrector. IEEE Trans Very Large Scale Integr Syst 20: 760-764.

GUO S, YU H, JIAN Z, LIU P, ZHU Y, GUO X, CHEN M, ISHIDA M & ZHOU H. 2014. A High-Capacity Low-Cost Layered Sodium Manganese Oxide Material as Cathode for Sodium-Ion Batteries. ChemSusChem 7: 2115-2119.

GUYOMARD D & TARASCON JM. 1995. High voltage stable liquid electrolytes for Li1+xMn2O4/carbon rocking-chair lithium batteries. J Power Sources 54: 92-98.

HASA I, VERRELLI R & HASSOUN J. 2015. Transition metal oxide-carbon composites as conversion anodes for sodium-ion battery. Electrochim Acta 173: 613-618.

HOLTSTIEGE F, BÄRMANN P, NÖLLE R, WINTER M & PLACKE T. 2018. Pre-Lithiation Strategies for Rechargeable Energy Storage Technologies: Concepts Promises and Challenges. Batteries 4: 4.

HONG XJ, TAN TX, GUO YK, TANG XY, WANG JY, QIN W & CAI YP. 2018. Confinement of polysulfides within bi-functional metal-organic frameworks for high performance lithium-sulfur batteries. Nanoscale 10: 2774-2780.

HOU H, QIU X, WEI W, ZHANG Y & JI X. 2017. Carbon Anode Materials for Advanced Sodium-Ion Batteries. Adv Energy Mater 7: 1-30.

HUANG H, LUO S, LIU C, YANG Y, ZHAI Y, CHANG L & LI M. 2019. Double-carbon coated Na3V2(PO4)3 as a superior cathode material for Na-ion batteries. Appl Surf Sci 487: 1159-1166.

HUANG Y ET AL. 2018. Activate metallic copper as high-capacity cathode for lithium-ion batteries via nanocomposite technology. Nano Energy 54: 59-65.

HUESO KB, ARMAND M & ROJO T. 2013. High temperature sodium batteries: status challenges and future trends. Energy Environ Sci 6: 734.

HU X, SUN X, YOO SJ, EVANKO B, FAN F, CAI S, ZHENG C, HU W & STUCKY GD. 2019. Nitrogen-rich hierarchically porous carbon as a high-rate anode material with ultra-stable cyclability and high capacity for capacitive sodium-ion batteries. Nano Energy 56: 828-839.

HWANG J, SETIADI CAHYADI H, CHANG W & KIM J. 2019. Uniform and ultrathin carbon-layer coated layered Na 2 Ti 3 O 7 and tunnel Na 2 Ti 6 O 13 hybrid with enhanced electrochemical performance for anodes in sodium ion batteries. J Supercrit Fluids 148: 116-129.

HWANG JY, MYUNG ST & SUN YK. 2017. Sodium-ion batteries: present and future. Chem Soc Rev 46: 3529-3614.

JACHE B & ADELHELM P. 2014. Use of graphite as a highly reversible electrode with superior cycle life for sodium-ion batteries by making use of co-intercalation phenomena. Angew Chemie - Int Ed 53: 10169-10173.

JANGID MK, VEMULAPALLY A, SONIA FJ, ASLAM M & MUKHOPADHYAY A. 2017. Feasibility of reversible electrochemical Na-storage and cyclic stability of amorphous silicon and silicon-graphene film electrodes. J Electrochem Soc 164: A2559-A2565.

JEONG SK, INABA M, ABE T & OGUMI Z. 2001. Surface Film Formation on Graphite Negative Electrode in Lithium-Ion Batteries: AFM Study in an Ethylene Carbonate-Based Solution. J Electrochem Soc 148: 989-993.

JI K ET AL. 2019. Lithium intercalation into bilayer graphene. Nat Commun 10: 1-10.

JIAO J, QIU W, TANG J, CHEN L & JING L. 2016. Synthesis of well-defined Fe3O4 nanorods/N-doped graphene for lithium-ion batteries. Nano Res 9: 1256-1266.

KASUGA T, HIRAMATSU M, HOSON A, SEKINO T & NIIHARA K. 1998. Formation of titanium oxide nanotube. Langmuir 14: 3160-3163.

KIM C, KIM I, KIM H, SADAN MK, YEO H, CHO G, AHN J, AHN J & AHN H. 2018. A self-healing Sn anode with an ultra-long cycle life for sodium-ion batteries. J Mater Chem A 6: 22809-22818.

KIM J, LEE KE, KIM KH, WI S, LEE S, NAM S, KIM C, KIM SO & PARK B. 2017. Single-layer graphene-wrapped Li4Ti5O12 anode with superior lithium storage capability. Carbon 114: 275-283.

KIM UH, KIM JH, HWANG JY, RYU HH, YOON CS & SUN YK. 2019. Compositionally and structurally redesigned high-energy Ni-rich layered cathode for next-generation lithium batteries. Mater Today 23: 26-36.

KLEIN F, JACHE B, BHIDE A & ADELHELM P. 2013. Conversion reactions for sodium-ion batteries. Phys Chem Chem Phys 15: 15876-15887.

KLEIN F, PINEDO R, BERKES BB, JANEK J & ADELHELM P. 2017. Kinetics and Degradation Processes of CuO as Conversion Electrode for Sodium-Ion Batteries: An Electrochemical Study Combined with Pressure Monitoring and DEMS. Phys Chem C 121: 8679-8691.

KO JS, DOAN-NGUYEN VVT, KIM HS, MULLER GA, SERINO AC, WEISS PS & DUNN BS. 2017. Na 2 Ti 3 O 7 nanoplatelets and nanosheets derived from a modified exfoliation process for use as a high-capacity sodium-ion negative electrode. ACS Appl Mater Interfaces 9: 1416-1425.

KOKETSU T, PAUL B, WU C, KRAEHNERT R, HUANG Y & STRASSER P. 2016. A lithium-tellurium rechargeable battery with exceptional cycling stability. J Appl Electrochem 46: 627-633.

KOO B, KIM H, CHO Y, LEE KT, CHOI NS & CHO J. 2012. A highly cross-linked polymeric binder for high-performance silicon negative electrodes in lithium ion batteries. Angew Chemie - Int Ed 51: 8762-8767.

KÜHNE M, PAOLUCCI F, POPOVIC J, OSTROVSKY PM, MAIER J & SMET JH. 2017. Ultrafast lithium diffusion in bilayer graphene. Nat Nanotechnol 12: 895-900.

KUMAR A, GHOSH A, ROY A, PANDA MR, FORSYTH M, MACFARLANE DR & MITRA S. 2019. High-energy density room temperature sodium-sulfur battery enabled by sodium polysulfide catholyte and carbon cloth current collector decorated with MnO2 nanoarrays. Energy Storage Mater 20: 196-202.

LEE B, PAEK E, MITLIN D & LEE SW. 2019. Sodium Metal Anodes: Emerging Solutions to Dendrite Growth. Chem Rev 119: 5416-5460.

LEE E & PERSSON KA. 2012. Li absorption and intercalation in single layer graphene and few layer graphene by first principles. Nano Lett 12: 4624-4628.

LEITE MM, MARTINS VL, VICHI FM & TORRESI RM. 2020. Electrochemistry of sodium titanate nanotubes as a negative electrode for sodium-ion batteries. Electrochim Acta 331: 135422.

LENCHUK O, ADELHELM P & MOLLENHAUER D. 2019. New insights into the origin of unstable sodium graphite intercalation compounds. Phys Chem Chem Phys 21: 19378-19390.

LI L ET AL. 2015a. Enhanced Cycling Stability of Lithium-Ion Batteries Using Graphene-Wrapped Fe3O4 -Graphene Nanoribbons as Anode Materials. Adv Energy Mater 5: 1500171.

LIM HD. et al. 2016. Rational design of redox mediators for advanced Li-O2 batteries. Nat Energy 1: 16066.

LI M, YU Y, LI J, CHEN B, KONAROV A & CHEN P. 2015b. Fabrication of graphene nanoplatelets-supported SiOx-disordered carbon composite and its application in lithium-ion batteries. J Power Sources 293: 976-982.

LI R, LIU Y, WANG Z & LI J. 2019a. A P2/O3 biphasic cathode material with highly reversibility synthesized by Sn-substitution for Na-ion batteries. Electrochim Acta 318: 14-22.

LI T, QIN A, YANG L, CHEN J, WANG Q, ZHANG D & YANG H. 2017a. In Situ Grown Fe 2 O 3 Single Crystallites on Reduced Graphene Oxide Nanosheets as High Performance Conversion Anode for Sodium-Ion Batteries. ACS Appl Mater Interfaces 9: 19900-19907.

LIU C, NEALE ZG & CAO G. 2016a. Understanding electrochemical potentials of cathode materials in rechargeable batteries. Mater Today 19: 109-123.

LIU N, LU Z, ZHAO J, MCDOWELL MT, LEE HW, ZHAO W & CUI Y. 2014a. A pomegranate-inspired nanoscale design for large-volume-change lithium battery anodes. Nat Nanotechnol 9: 187-192.

LIU T, DAI C, JIA M, LIU D, BAO S, JIANG J, XU M & LI CM. 2016b. Selenium Embedded in Metal-Organic Framework Derived Hollow Hierarchical Porous Carbon Spheres for Advanced Lithium-Selenium Batteries. ACS Appl Mater Interfaces 8: 16063-16070.

LIU T ET AL. 2018. The Effect of Water on Quinone Redox Mediators in Nonaqueous Li-O 2 Batteries. J Am Chem Soc 140: 1428-1437.

LIU X. H, ZHONG L, HUANG S, MAO SX, ZHU T & HUANG JY. 2012. Size-dependent fracture of silicon nanoparticles during lithiation. ACS Nano 6: 1522-1531.

LIU Y, FAN X, ZHANG Z, WU HH, LIU D, DOU A, SU M, ZHANG Q & CHU D. 2019a. Enhanced Electrochemical Performance of Li-Rich Layered Cathode Materials by Combined Cr Doping and LiAlO 2 Coating. ACS Sustain Chem Eng 7: 2225-2235.

LIU Y, HUANG K, LUO H, LI H, QI X & ZHONG J. 2014b. Nitrogen-doped graphene-Fe3O4 architecture as anode material for improved Li-ion storage. RSC Adv 4: 17653-17659.

LIU Y, MERINOV BV & GODDARD WA. 2016c. Origin of low sodium capacity in graphite and generally weak substrate binding of Na and Mg among alkali and alkaline earth metals. Proc Natl Acad Sci 113: 3735-3739.

LIU Y, ZHANG N, JIAO L & CHEN J. 2015. Tin Nanodots Encapsulated in Porous Nitrogen-Doped Carbon

Nanofibers as a Free-Standing Anode for Advanced Sodium-Ion Batteries. Adv Mater 27: 6702-6707.

LIU Z, YU Q, ZHAO Y, HE R, XU M, FENG S, LI S, ZHOU L & MAI L. 2019b. Silicon oxides: A promising family of anode materials for lithium-ion batteries. Chem Soc Rev 48: 285-309.

LI W, SONG B & MANTHIRAM A. 2017b. High-voltage positive electrode materials for lithium-ion batteries. Chem Soc Rev 46: 3006-3059.

LI Y, LU Y, ADELHELM P, TITIRICI MM & HU YS. 2019b. Intercalation chemistry of graphite: alkali metal ions and beyond. Chem Soc Rev 48: 4655-4687.

LUO W, BOMMIER C, JIAN Z, LI X, CARTER R, VAIL S, LU Y, LEE JJ & JI X. 2015. Low-surface-area hard carbon anode for Na-ion batteries via graphene oxide as a dehydration agent. ACS Appl Mater Interfaces 7: 2626-2631.

LU X, XIA G, LEMMON JP & YANG Z. 2010. Advanced materials for sodium-beta alumina batteries: Status challenges and perspectives. J Power Sources 195: 2431-2442.

LV P, ZHAO H, GAO C, DU Z, WANG J & LIU X. 2015. SiOx-C dual-phase glass for lithium ion battery anode with high capacity and stable cycling performance. J Power Sources 274: 542-550.

LYU Z ET AL. 2015. Hierarchical carbon nanocages confining high-loading sulfur for high-rate lithium-sulfur batteries. Nano Energy 12: 657-665.

MA C, SHI J, ZHAO Y, SONG N & WANG Y. 2017a. A novel porous reduced microcrystalline graphene oxide supported Fe3O4@C nanoparticle composite as anode material with excellent lithium storage performances. Chem Eng J 326: 507-517.

MACFARLANE DR ET AL. 2016. Ionic liquids and their solid-state analogues as materials for energy generation and storage. Nat Rev Mater 1: 15005.

MA L, CHEN R, ZHU G, HU Y, WANG Y, CHEN T, LIU J & JIN Z. 2017b. Cerium Oxide Nanocrystal Embedded Bimodal Micromesoporous Nitrogen-Rich Carbon Nanospheres as Effective Sulfur Host for Lithium – Sulfur Batteries. ACS Nano 11: 7274-7283.

MARTHA SK, HAIK O, ZINIGRAD E, EXNAR I, DREZEN T, MINERS JH & AURBACH D. 2011. On the Thermal Stability of Olivine Cathode Materials for Lithium-Ion Batteries. J Electrochem Soc 158: A1115-A1122.

MARTINS VL & TORRESI RM. 2020. Water-in-salt electrolytes for high voltage aqueous electrochemical energy storage devices. Curr Opin Electrochem 21: 62-68.

MCCLOSKEY BD, SPEIDEL A, SCHEFFLER R, MILLER DC, VISWANATHAN V, HUMMELSHØJ JS, NØRSKOV JK & LUNTZ AC. 2012. Twin problems of interfacial carbonate formation in nonaqueous Li-O 2 batteries. J Phys Chem Lett 3: 997-1001.

MEDENBACH L & ADELHELM P. 2017. Cell Concepts of Metal-Sulfur Batteries (Metal = Li Na K Mg): Strategies for Using Sulfur in Energy Storage Applications. Top Curr Chem 375: 81.

MEINI S, ELAZARI R, ROSENMAN A, GARSUCH A & AURBACH D. 2014. The Use of Redox Mediators for Enhancing Utilization of Li 2 S Cathodes for Advanced Li-S Battery Systems. J Phys Chem Lett 5: 915-918.

MENDIBOURE A, DELMAS C & HAGENMULLER P. 1985. Electrochemical intercalation and deintercalation of NaxMnO2 bronzes. J Solid State Chem 57: 323-331.

MIZUSHIMA K, JONES P, WISEMAN P & GOODENOUGH JB. 1980. LixCoO2 (0<x<-1): A new cathode material for batteries of high energy density. Mater Res Bull 15: 783-789.

MORIWAKE H, KUWABARA A, FISHER CAJ & IKUHARA Y. 2017. Why is sodium-intercalated graphite unstable? RSC Adv 7: 36550-36554.

NAYAK PK, YANG L, BREHM W & ADELHELM P. 2018. From Lithium-Ion to Sodium-Ion Batteries: Advantages Challenges and Surprises. Angew Chemie - Int Ed 57: 102-120.

NITTA N, WU F, LEE JT & YUSHIN G. 2015. Li-ion battery materials: present and future. Mater Today 18: 252-264.

PADHI AK. 1997. Phospho-olivines as Positive-Electrode Materials for Rechargeable Lithium Batteries. J Electrochem Soc 144: 1188.

PAN M, LIU X, LIU H & CHEN Y. 2016. Ultrafine Si/C-graphite composite anode materials with improved cyclic performance. Mater Lett 178: 252-255.

PELED E, GOLODNITSKY D, ARDEL G & ESHKENAZY V. 1995. The sei model-application to lithium-polymer electrolyte batteries. Electrochim Acta 40: 2197-2204.

PIPER DM, YERSAK TA, SON SB, KIM SC, KANG CS, OH KH, BAN C, DILLON AC & LEE SH. 2013. Conformal coatings of cyclized-PAN for mechanically resilient Si nano-composite anodes. Adv Energy Mater 3: 697-702.

PIPER DM ET AL. 2015. Stable silicon-ionic liquid interface for next-generation lithium-ion batteries. Nat Commun 6: 6230.

POLLAK E, GENG B, JEON KJ, LUCAS IT, RICHARDSON TJ, WANG F & KOSTECKI R. 2010. The interaction of Li+ with single-layer and few-layer graphene. Nano Lett 10: 3386-3388.

QIAN L, LAN JL, XUE M, YU Y & YANG X. 2017. Two-step ball-milling synthesis of a Si/SiOx/C composite electrode for lithium ion batteries with excellent long-term cycling stability. RSC Adv 7: 36697-36704.

RAMESH TN, LEE KT, ELLIS BL & NAZAR LF. 2010. Tavorite Lithium Iron Fluorophosphate Cathode Materials: Phase Transition and Electrochemistry of LiFePO4F-Li2FePO4F. Electrochem Solid-State Lett 13: A43.

RAMOS A, CAMEÁN I, CUESTA N & GARCÍA AB. 2015. Is single layer graphene a promising anode for sodium-ion batteries? Electrochim Acta 178: 392-397.

ROUGIER A, GRAVEREAU P & DELMAS C. 1996. Optimization of the Composition of the Li1-zNi1+zO2 Electrode Materials: Structural Magnetic and Electrochemical Studies. J Electrochem Soc 143: 1168.

SANCHEZ-RAMIREZ N, ASSRESAHEGN BD, TORRESI RM & BÉLANGER D. 2020. Producing high-performing silicon anodes by tailoring ionic liquids as electrolytes. Energy Storage Mater 25: 477-486.

SENGUTTUVAN P, ROUSSE G, SEZNEC V, TARASCON JM & PALACÍN MR. 2011. Na2Ti3O7 : Lowest Voltage Ever Reported Oxide Insertion Electrode for Sodium Ion Batteries. Chem Mater 23: 4109-4111.

SHAO J, LI X, ZHANG L, QU Q & ZHENG H. 2013. Core-shell sulfur@polypyrrole composites as high-capacity materials for aqueous rechargeable batteries. Nanoscale 5: 1460.

SHEN X, LIU H, CHENG XB, YAN C & HUANG JQ. 2018. Beyond lithium ion batteries: Higher energy density battery systems based on lithium metal anodes. Energy Storage Mater 12: 161-175.

SILVA SP, SILVA PRC, URBANO A & SCARMINIO J. 2016. Analysis Of A Commercial Portable Lithium-Ion Battery Under Low Current Charge-Discharge Cycles. Quim Nova 39: 901-905.

SLATER MD, KIM D, LEE E & JOHNSON CS. 2013. Sodium-Ion Batteries. Adv Funct Mater 23: 947-958.

SONG JP ET AL. 2019a. MOF-derived nitrogen-doped core-shell hierarchical porous carbon confining selenium for advanced lithium-selenium batteries. Nanoscale 11: 6970-6981.

SONG K, LIU C, MI L, CHOU S, CHEN W & SHEN C. 2019b. Recent Progress on the Alloy-Based Anode for Sodium-Ion Batteries and Potassium-Ion Batteries. Small 1903194.

STEVENS DA & DAHN JR. 2000. High Capacity Anode Materials for Rechargeable Sodium-Ion Batteries. J Electrochem Soc 147: 1271.

STRATFORD JM, ALLAN PK, PECHER O, CHATER PA & GREY CP. 2016. Mechanistic insights into sodium storage in hard carbon anodes using local structure probes. Chem Commun 52: 12430-12433.

SUN Y, GUO S & ZHOU H. 2019. Exploration of Advanced Electrode Materials for Rechargeable Sodium-Ion Batteries. Adv Energy Mater 9: 1800212.

SUO L, BORODIN O, GAO T, OLGUIN M, HO J, FAN X, LUO C, WANG C & XU K. 2015. "Water-in-salt" electrolyte enables high-voltage aqueous lithium-ion chemistries. Science 350: 938-943.

SUO L, HAN F, FAN X, LIU H, XU K & WANG C. 2016. "Water-in-Salt" electrolytes enable green and safe Li-ion batteries for large scale electric energy storage applications. J Mater Chem A 4: 6639-6644.

TALAIE E, BONNICK P, SUN X, PANG Q, LIANG X & NAZAR LF. 2017. Methods and Protocols for Electrochemical Energy Storage Materials Research. Chem Mater 29: 90-105.

TAO Y, WEI Y, LIU Y, WANG J, QIAO W, LING L & LONG D. 2016. Kinetically-enhanced polysulfide redox reactions by Nb 2 O 5 nanocrystals for high-rate lithium-sulfur battery. Energy Environ Sci 9: 3230-3239.

THACKERAY MM, DAVID WIF, BRUCE PG & GOODENOUGH JB. 1983. Lithium insertion into manganese spinels. Mater Res Bull 18: 461-472.

THACKERAY MM, JOHNSON PJ, DE PICCIOTTO LA, BRUCE PG & GOODENOUGH JB. 1984. Electrochemical extraction of lithium from LiMn2O4. Mater Res Bull 19: 179-187.

TORRESI RM, CORRÊA CM, BENEDETTI TM & MARTINS VL. 2018. Tailoring Transport Properties Aiming for Versatile Ionic Liquids and Poly(Ionic Liquids) for Electrochromic and Gas Capture Applications. In: Polym Ion Liq Cambridge: Royal Society of Chemistry. 342-380.

TU J, ZHAO XB, CAO GS, ZHUANG DG, ZHU TJ & TU JP. 2006. Enhanced cycling stability of LiMn2O4 by surface modification with melting impregnation method. Electrochim Acta 51: 6456-6462.

VALVO M, LINDGREN F, LAFONT U, BJÖREFORS F & EDSTRÖM K. 2014. Towards more sustainable negative electrodes in Na-ion batteries via nanostructured iron oxide. J Power Sources 245: 967-978.

WANG B, RUAN T, CHEN Y, JIN F, PENG L, ZHOU Y, WANG D & DOU S. 2020. Graphene-based composites for electrochemical energy storage. Energy Storage Mater 24: 22-51.

WANG F ET AL. 2016. Stabilizing high voltage LiCoO2 cathode in aqueous electrolyte with interphase-forming additive. Energy Environ Sci 9: 3666-3673.

WANG J, ENG C, CHEN-WIEGART YK & WANG J. 2015a. Probing three-dimensional sodiation-desodiation equilibrium in sodium-ion batteries by in situ hard X-ray nanotomography. Nat Commun 6: 7496.

WANG L, DONG Z, WANG D, ZHANG F & JIN J. 2013. Covalent Bond Glued Sulfur Nanosheet-Based Cathode Integration for Long-Cycle-Life Li-S Batteries. Nano Lett 13: 6244-6250.

WANG QC, QIU QQ, XIAO N, FU ZW, WU XJ, YANG XQ & ZHOU YN. 2018. Tunnel-structured Na0.66[Mn0.66Ti0.34]O2-F (x<0.1) cathode for high performance sodium-ion batteries. Energy Storage Mater 15: 1-7.

WANG S, WANG W, ZHAN P, YUAN Y, JIAO K, JIAO H & JIAO S. 2015b. 3D flower-like NaHTi 3 O 7 nanotubes as high-performance anodes for sodium-ion batteries. J Mater Chem A 3: 16528-16534.

WANG Y, ZAGHIB K, GUERFI A, BAZITO FFC, TORRESI RM & DAHN JR. 2007. Accelerating rate calorimetry studies of the reactions between ionic liquids and charged lithium ion battery electrode materials. Electrochim Acta 52: 6346-6352.

WANG Z, WANG B, YANG Y, CUI Y, WANG Z, CHEN B & QIAN G. 2015c. Mixed-Metal-Organic Framework with Effective Lewis Acidic Sites for Sulfur Confinement in High-Performance Lithium-Sulfur Batteries. ACS Appl Mater Interfaces 7: 20999-21004.

WEI S, XU S, AGRAWRAL A, CHOUDHURY S, LU Y, TU Z, MA L & ARCHER LA. 2016. A stable room-temperature sodium-sulfur battery. Nat Commun 7: 11722.

WHITTINGHAM MS. 1978. Chemistry of intercalation compounds: Metal guests in chalcogenide hosts. Prog Solid State Chem 12: 41-99.

WILD M, O'NEILL L, ZHANG T, PURKAYASTHA R, MINTON G, MARINESCU M & OFFER GJ. 2015. Lithium sulfur batteries a mechanistic review. Energy Environ Sci 8: 3477-3494.

WINTER M & BRODD RJ. 2004. What Are Batteries Fuel Cells and Supercapacitors? Chem Rev 104: 4245-4270.

WORTHINGTON MJH, KUCERA RL & CHALKER JM. 2017. Green chemistry and polymers made from sulfur. Green Chem 19: 2748-2761.

WU F & YUSHIN G. 2017. Conversion cathodes for rechargeable lithium and lithium-ion batteries. Energy Environ Sci 10: 435-459.

WU H, ZHENG G, LIU N, CARNEY TJ, YANG Y & CUI Y. 2012a. Engineering Empty Space between Si Nanoparticles for Lithium-Ion Battery Anodes. Nano Lett 12: 904-909.

WU H ET AL. 2012b. Stable cycling of double-walled silicon nanotube battery anodes through solid-electrolyte interphase control. Nat Nanotechnol 7: 310-315.

WU H & CUI Y. 2012. Designing nanostructured Si anodes for high energy lithium ion batteries. Nano Today 7: 414-429.

WU J ET AL. 2015a. Multilayered silicon embedded porous carbon/graphene hybrid film as a high performance anode. Carbon 84: 434-443.

WU W, SHI J, LIANG Y, LIU F, PENG Y & YANG H. 2015b. A low-cost and advanced SiOx-C composite with hierarchical structure as an anode material for lithium-ion batteries. Phys Chem Chem Phys 17: 13451-13456.

XIAO B, ROJO T & LI X. 2019. Hard Carbon as Sodium-Ion Battery Anodes: Progress and Challenges. ChemSusChem 12: 133-144.

XUE Z, HE D & XIE X. 2015. Poly(ethylene oxide)-based electrolytes for lithium-ion batteries. J Mater Chem A 3: 19218-19253.

XU J, CHEN J, TAO L, TIAN Z, ZHOU S, ZHAO N & WONG CP. 2019a. Investigation of Na3V2(PO4)2O2F as a sodium ion battery cathode material: Influences of morphology and voltage window. Nano Energy 60: 510-519.

XU ZL, YOON G, PARK KY, PARK H, TAMWATTANA O, JOO KIM S, SEONG WM & KANG K. 2019b. Tailoring sodium intercalation in graphite for high energy and power sodium ion batteries. Nat Commun 10: 1-10.

YABUUCHI N, KUBOTA K, DAHBI M & KOMABA S. 2014. Research Development on Sodium-Ion Batteries. Chem Rev 114: 11636-11682.

YAN Z, LIU L, SHU H, YANG X, WANG H, TAN J, ZHOU Q, HUANG Z & WANG X. 2015. A tightly integrated sodium titanate-carbon composite as an anode material for rechargeable sodium ion batteries. J Power Sources 274: 8-14.

YANG C ET AL. 2017a. Unique aqueous Li-ion/sulfur chemistry with high energy density and reversibility. Proc Natl Acad Sci 114: 6197-6202.

YANG C ET AL. 2019a. Aqueous Li-ion battery enabled by halogen conversion-intercalation chemistry in graphite. Nature 569: 245-250.

YANG H, XU R & YU Y. 2019b. A facile strategy toward sodium-ion batteries with ultra-long cycle life and high initial Coulombic Efficiency: Free-standing porous carbon nanofiber film derived from bacterial cellulose. Energy Storage Mater 22: 105-112.

YANG Y ET AL. 2017b. "Protrusions" or "holes" in graphene: Which is the better choice for sodium ion storage? Energy Environ Sci 10: 979-986.

YOO H ET AL. 2018. Si Nanocrystal-Embedded SiO x nanofoils: Two-Dimensional Nanotechnology-Enabled High Performance Li Storage Materials. Sci Rep 8: 1-9.

YOON G, KIM H, PARK I & KANG K. 2017. Conditions for Reversible Na Intercalation in Graphite: Theoretical Studies on the Interplay Among Guest Ions Solvent and Graphite Host. Adv Energy Mater 7: 1601519.

YOSHINO A. 2000. Development of Lithium Ion Battery. Mol Cryst Liq Cryst Sci Technol Sect A Mol Cryst Liq Cryst 340: 425-429.

ZHANG B, ROUSSE G, FOIX D, DUGAS R, CORTE DAD & TARASCON JM. 2016a. Microsized Sn as Advanced Anodes in Glyme-Based Electrolyte for Na-Ion Batteries. Adv Mater 28: 9824-9830.

ZHANG H ET AL. 2019. Highly Elastic Binders Incorporated with Helical Molecules Improving the Electrochemical Stability of Black Phosphorous Anode for Sodium Ion Batteries. Batter Supercaps c: 1-8.

ZHANG H, HUANG Y, MING H, CAO G, ZHANG W, MING J & CHEN R. 2020. Recent advances in nanostructured carbon for sodium-ion batteries. J Mater Chem A 8: 1604-1630.

ZHANG L, LIU X, ZHAO Q, DOU S, LIU H, HUANG Y & HU X. 2016b. Si-containing precursors for Si-based anode materials of Li-ion batteries: A review. Energy Storage Mater 4: 92-102.

ZHANG SS. 2006. A review on electrolyte additives for lithium-ion batteries. J Power Sources 162: 1379-1394.

ZHANG Z, HU L, WU H, WENG W, KOH M, REDFERN PC, CURTISS LA & AMINE K. 2013. Fluorinated electrolytes for 5 V lithium-ion battery chemistry. Energy Environ Sci 6: 1806-1810.

ZHAO Y, SONG Z, LI X, SUN Q, CHENG N, LAWES S & SUN X. 2016. Metal organic frameworks for energy storage and conversion. Energy Storage Mater 2: 35-62.

ZHENG X, BOMMIER C, LUO W, JIANG L, HAO Y & HUANG Y. 2019. Sodium metal anodes for room-temperature sodium-ion batteries: Applications challenges and solutions. Energy Storage Mater 16: 6-23.

ZHOU J, LI R, FAN X, CHEN Y, HAN R, LI W, ZHENG J, WANG B & LI X. 2014. Rational design of a metal-organic framework host for sulfur storage in fast long-cycle Li-S batteries. Energy Environ Sci 7: 2715.

ZHOU J ET AL. 2015. The impact of the particle size of a metal-organic framework for sulfur storage in Li-S batteries. J Mater Chem A 3: 8272-8275.

ZHOU Z, XIAO H, ZHANG F, ZHANG X & TANG Y. 2016. Solvothermal synthesis of Na2Ti3O7nanowires embedded in 3D graphene networks as an anode for high-performance sodium-ion batteries. Electrochim Acta 211: 430-436.

How to cite

MARTINS VL ET AL. 2020. An Overview on the Development of Electrochemical Capacitors and Batteries – part II. An Acad Bras Cienc 92: e20200800. DOI 10.1590/0001-3765202020200800.

Manuscript received on May 24, 2020; accepted for publication on May 25, 2020

VITOR L. MARTINS[1]
https://orcid.org/0000-0002-8824-7328

HERBERT R. NEVES[1,2]
https://orcid.org/0000-0001-7756-5278

IVONNE E. MONJE[1]
https://orcid.org/0000-0002-1220-3580

MARINA M. LEITE[1]
https://orcid.org/0000-0002-4569-5673

PAULO F.M. DE OLIVEIRA[1]
https://orcid.org/0000-0003-4854-5352

RODOLFO M. ANTONIASSI[1]
https://orcid.org/0000-0002-7027-7860

SUSANA CHAUQUE[1]
https://orcid.org/0000-0003-3950-6538

WILLIAM G. MORAIS[1]
https://orcid.org/0000-0001-6686-8687

EDUARDO C. MELO[1]
https://orcid.org/0000-0002-3489-9865

THIAGO T. OBANA[1]
https://orcid.org/0000-0002-0644-9883

BRENO L. SOUZA[1]
https://orcid.org/0000-0001-6774-2664

ROBERTO M. TORRESI[1]
https://orcid.org/0000-0003-4414-5431

[1]Universidade de São Paulo, Depto. Química Fundamental, Instituto de Química, Av. Prof. Lineu Prestes, 748, 05508-000 São Paulo, SP, Brazil

[2]Catarinense Federal Institute for Education Science and Technology – IFC, Campus Araquari, Rodovia BR280, Km 27, s/n, C.P. 21, 89245-000 Araquari, SC, Brazil

Correspondence to: **Roberto Manuel Torresi**
E-mail: rtorresi@iq.usp.br

Author contributions

VLM: Conceptualization, Writing original draft preparation and Writing-Reviewing and Editing. HRN, IEM, PMO, RMA, SC, WGM, EC, TTO, BLS: Writing original draft preparation. MML: Writing original draft preparation and Reviewing last version. RMT: Conceptualization, Supervision, Writing-Reviewing last version.